NACA RM A52D01a

NACA

RESEARCH MEMORANDUM

EFFECTS OF PROPELLER-SPINNER JUNCTURE ON THE PRESSURE-
RECOVERY CHARACTERISTICS OF AN NACA 1-SERIES D-TYPE
COWL IN COMBINATION WITH A FOUR-BLADE SINGLE-
ROTATION PROPELLER AT MACH NUMBERS UP TO
0.83 AND AT AN ANGLE OF ATTACK OF 0°

By Robert I. Sammonds and Ashley J. Molk

Ames Aeronautical Laboratory
Moffett Field, Calif.

CLASSIFIED DOCUMENT

This material contains information affecting the National Defense of the United States within the meaning
of the espionage laws, Title 18, U.S.C., Secs. 793 and 794, the transmission or revelation of which in any
manner to an unauthorized person is prohibited by law.

NATIONAL ADVISORY COMMITTEE
FOR AERONAUTICS
WASHINGTON
June 24, 1952

NACA RM A52D01a

NATIONAL ADVISORY COMMITTEE FOR AERONAUTICS

RESEARCH MEMORANDUM

EFFECTS OF PROPELLER-SPINNER JUNCTURE ON THE PRESSURE-RECOVERY
CHARACTERISTICS OF AN NACA 1-SERIES D-TYPE COWL IN
COMBINATION WITH A FOUR-BLADE SINGLE-ROTATION
PROPELLER AT MACH NUMBERS UP TO 0.83
AND AT AN ANGLE OF ATTACK OF 0°

By Robert I. Sammonds and Ashley J. Molk

SUMMARY

An investigation has been conducted to determine the effects of two
types of propeller-spinner junctures on the pressure-recovery character-
istics of an NACA 1-series D-type cowl with an NACA 1-series spinner,
in combination with a four-blade single-rotation propeller. Ram-recovery
ratio was measured in the duct with the propeller removed and with the
propeller operating. The two types of propeller-spinner junctures tested
consisted of an "ideal" juncture, formed by extending the propeller blade
to the spinner surface and sealing all gaps, and a platform juncture,
which consisted of an airfoil-shaped land integral with the spinner sur-
face with provisions for changing the propeller-blade angle. The data
were obtained at inlet-velocity ratios from 0.26 to 1.33 at Mach numbers
from 0.20 to 0.83 at a Reynolds number of 1.77 million, based on maximum
diameter of the cowl. The effects of the two types of propeller-spinner
junctures were investigated at various advance-diameter ratios for
propeller blade angles of 60°, 50°, and 40°, with the platform juncture
being set to aline with the propeller blade at a propeller blade angle
of 60°.

With the propeller removed there was no effect of Mach number on the
pressure recovery, and for inlet-velocity ratios below 0.4 the recoveries
decreased rapidly. The addition of the propeller resulted in a decrease
in the recovery at a given inlet-velocity ratio and Mach number, and also
increased the minimum inlet-velocity ratio necessary to avoid excessive
losses.

Little difference was obtained in the ram-recovery ratio for the
ideal and platform junctures, except for a propeller blade angle of 40°,
where the platform juncture was superior to the ideal juncture.

With the propeller operating ahead of the inlet, the ram-recovery
ratio increased with increasing inlet-velocity ratio up to an inlet-
velocity ratio of 0.8, except for the platform juncture with the
40° propeller blade angle. Above this value, inlet-velocity ratio had
little or no effect on the ram-recovery ratio. For the platform junc-
ture with the propeller blade angle at 40°, the pressure recoveries
were relatively constant above an inlet-velocity ratio of 0.6. Below
an inlet-velocity ratio of 0.6, the recoveries decreased rapidly.

The effect of advance-diameter ratio and the effect of Mach number
(propeller operating) on the pressure recoveries was quite small.

INTRODUCTION

A growing interest in the utilization of the turbine-propeller
type of power plant for moderately high-speed long-range airplanes has
led to a need for data on the effects of the propeller and the propeller-
spinner junctures on the pressure-recovery characteristics of a cowling-
spinner combination. The efficiency of the air-induction system has a
large effect on the power and the fuel economy of a gas-turbine engine
(reference 1). In the case of the cowling-spinner-propeller combination,
the induction efficiency can be quite low as a result of interference
effects of the propeller blade shanks and pressure losses due to the
spinner boundary layer.

Previous investigations at low speeds (references 2 and 3) have
been conducted to determine the effect of the spinner and the propeller
on the pressure recoveries in the duct. The design charts available in
reference 2 were used in the present investigation to select a cowling-
spinner combination having a high critical Mach number and a high intake
efficiency.

The purpose of this investigation was to study the effects of two
types of propeller-spinner junctures, in combination with a four-blade
single-rotation propeller, on pressure-recovery characteristics of an
NACA 1-series D-type cowl with an NACA 1-series elliptical spinner.
The investigation was conducted at Mach numbers up to 0.83 for various
advance-diameter and inlet-velocity ratios in order to determine the
relationship of these parameters to the recoveries in the duct. These
tests were made with the cowl at an angle of attack of 0°.

The results of this investigation conducted in the Ames 12-foot
pressure wind tunnel are presented herein.

SYMBOLS

A   cross-sectional area in a plane perpendicular to the model center line, square feet

a   speed of sound, feet per second

b   propeller blade chord, feet

c_{l_d} propeller blade section design lift coefficient

D   propeller diameter, feet

H   total pressure, pounds per square foot

$\dfrac{H_1-p_0}{H_0-p_0}$ ram-recovery ratio

h   propeller-blade thickness, feet

M   Mach number $\left(\dfrac{V}{a}\right)$

m   mass flow $(\rho A V)$, slugs per second

$\dfrac{m_1}{m_0}$ mass-flow ratio $\left(\dfrac{\rho_1 A_1 V_1}{\rho_0 A_1 V_0}\right)$

n   propeller rotational speed, revolutions per second

p   static pressure, pounds per square foot

R   maximum radius of propeller measured from the center of rotation $\left(\dfrac{D}{2}\right)$, feet

r   radius from center of rotation, feet

V   velocity, feet per second

$\dfrac{V_0}{nD}$ advance-diameter ratio

$\dfrac{V_1}{V_0}$ inlet-velocity ratio

X   total length along the longitudinal axis of any component of the
           model such as the cowl, spinner, or inner lip, inches

x   distance along the longitudinal axis from any reference, such
           as the leading edge of the cowl, spinner, or inner lip, inches

ρ mass density of air, slugs per cubic foot

β propeller blade angle at 0.75 R

Subscripts

o   free stream

1   ram-recovery rake location

c   cowl

i   inner lip

s   spinner

MODEL

The 1/5-scale model, used in this investigation, was mounted in
the test section of the Ames 12-foot pressure wind tunnel as shown in
figure 1. A sketch of the general model arrangement, showing the princi-
pal model dimensions, is shown in figure 2. Coordinates for the model
cowling-spinner combination are shown in table I. The four-blade
single-rotation propeller was driven by means of a 1000-horsepower
electric motor.

Design Conditions

The model investigated simulates a cowling-spinner combination for
a turboprop installation having the following design requirements:

Operating altitude, feet 35,000
Flight Mach number (cruise). 0.80
Power plant. . . . . Turboprop
Power requirements (design altitude and speed),
    horsepower . . . . 5,000 to 6,000
Engine air flow, pounds per second 40
Maximum cowling diameter, inches 70

Cowling-Spinner Combination

The cowling-spinner combination, selected to comply with the design condition, consisted of an NACA 1-46.5-047 spinner and an NACA 1-62.8-070 D-cowl. The 1-46.5-047 spinner was chosen as the smallest spinner which would enclose a representative propeller hub assembly. The NACA 1-62.8-070 D-cowl was selected, with an NACA 1-series inner lip to avoid separation at the high inlet-velocity ratios, in accordance with design charts of reference 2, for a design critical Mach number of 0.75 and a design inlet-velocity ratio of 0.42. Coordinates for the 1/5-scale model, as shown in table I, were calculated from the NACA 1-series nondimensional coordinates of reference 2. In order to vary the inlet-velocity ratio, a sliding throttle was incorporated in the duct (fig. 2).

Propeller

The NACA 4-(5)(05)-041 four-blade single-rotation propeller was designed, in accordance with the method of reference 4, to operate at an advance-diameter ratio of 3.7 and a blade angle of 60° (0.75 R) at the design condition. This design was for a full-scale propeller, 20 feet in diameter, having NACA 16-series sections. Plan-form and blade-form curves for the propeller are shown in figure 3.

Propeller-Spinner Junctures

Two types of propeller-spinner junctures were tested. These were designated as an ideal juncture and a platform juncture, both having a thickness-chord ratio (h/b) of approximately 0.24 and the coordinates of an NACA 16-series airfoil section. The ideal type of propeller-spinner juncture (fig. 4) was formed by extending the propeller blade by use of filler blocks to the surface of the spinner and sealing all gaps. The discontinuity, noticeable in figure 4, between the propeller blade and the filler block resulted from designing the filler block from the extended b/D curve of figure 3 with the maximum diameter being that of the propeller shank. In order to change the blade angle, a separate set of filler blocks were required for each blade-angle setting. The platform juncture (fig. 5) consists of an airfoil-shaped land that is mounted integrally with the spinner at a predetermined angle. This angle was selected so that the propeller shank would be in alinement with the land at the design propeller blade angle of 60° measured at the 0.75 radius. The gap (0.025 in. between the land and the propeller

blade) was located outside the spinner boundary layer in order to
increase the pressure recoveries (reference 3).

Instrumentation of the Model

In order to determine the ram-recovery ratio and inlet-velocity
ratio, six survey rakes were located in the duct at a station 2.8 inches
aft of the leading edge of the cowl. These consisted of four shielded
total-head rakes located 90° apart and two static-pressure rakes
located 180° apart, as shown in figure 6.

Total-head rakes.- Each total-head rake consisted of eight tubes
disposed radially across the duct and spaced in such a manner that each
tube was located in the center of an area equal to one-thirty-second of
the total duct area.

In order to eliminate the effects of air flow rotation on the rake,
the total-head rakes were shielded. It was felt that the shielding was
only required in one direction, normal to a circumferential rotation,
due to the rake being located far enough back in the duct so that any
angularity of the flow due to the inner lip was eliminated. On this
basis, the shielding was designed, in accordance with reference 5, as
two cambered airfoils spanning the duct from the inner surface to the
outer surface (fig. 6). Calibration of these rakes indicated that
the rakes were reliable within 1 percent of the impact pressure at angles
of attack up to 40° for Mach numbers up to 0.85.

Static-pressure rakes.- The static-pressure rakes consisted of
eight tubes disposed radially across the duct with the tubes being
located at the same radial stations used for the total-head rake. These
tubes were alternately displaced circumferentially to prevent interference
in the flow about the individual tubes. No attempt was made to calibrate
the static rakes as they were considered to be within the accuracy
required for the calculation of the inlet-velocity ratio.

TESTS AND REDUCTION OF DATA

Pressure-recovery surveys were conducted with the propeller removed
and with the propeller installed (ideal and platform propeller-spinner
junctures). With the propeller removed, tests were made at inlet-velocity
ratios ranging from 0.26 to 1.33 and for Mach numbers from 0.20 to 0.83.
The tests with the propeller operating were made at three blade angles
for various inlet-velocity ratios, Mach numbers, and advance-diameter
ratios, as tabulated:

Propeller blade angle, degrees (β, 0.75 R)	Juncture type	Mach number, M_O	Inlet-velocity ratio, V_1/V_O	Advance-diameter ratio, V_O/nD
60	Ideal	0.83	0.31 to 1.00	3.20 to 4.15
60		.79	.31 to 1.02	3.17 to 4.29
60		.69	.31 to 1.10	3.06 to 4.36
60		.59	.42 to 1.27	2.90 to 4.50
50		.59	.39 to 1.29	2.44 to 2.96
50		.39	.39 to 1.28	2.00 to 3.05
40		.39	.37 to 1.26	1.67 to 2.10
40		.30	.36 to 1.26	1.50 to 2.12
40		.20	.37 to 1.24	1.30 to 2.10
60	Platform	.83	.30 to .84	3.15 to 4.16
60		.79	.27 to .80	3.18 to 4.24
60		.69	.30 to .84	3.05 to 4.42
60		.59	.32 to .81	2.95 to 4.44
50		.59	.37 to 1.27	2.36 to 2.96
50		.39	.39 to 1.27	2.06 to 3.00
40		.39	.38 to 1.28	1.68 to 2.10
40		.30	.35 to 1.26	1.50 to 2.15
40		.20	.41 to 1.24	1.30 to 2.10

Conversion of the inlet-velocity ratio to mass-flow ratio (m_1/m_O) can be readily accomplished by the use of figure 4 of reference 6. The thrust coefficient (T_c) varied from 0 to 0.040 for a propeller blade angle of 60°, 0 to 0.066 for 50°, and 0 to 0.143 for 40°.

All of the tests were conducted at an angle of attack of 0° and a Reynolds number of 1.77 million, based on the maximum diameter of the cowl.

The inlet-velocity ratios were calculated in accordance with the method of reference 6. The ram-recovery ratios were obtained from an arithmetic average of the total-pressure readings, which is equivalent to an area-weighted average. For the radial distributions, the recoveries were obtained from an average of the four total-pressure readings at each respective radial location, and for the remaining figures the recoveries were obtained from an average of all 32 total-pressure readings.

The effects of constriction due to the tunnel walls on the free-stream Mach number and dynamic pressure were estimated by the method of reference 7.

RESULTS

The data have been presented for the two types of propeller-spinner junctures in such a manner that they are readily comparable for the parameters investigated.

Ram-recovery ratios across the duct are shown in figure 7 for various inlet-velocity ratios and Mach numbers, with the propeller removed. Figures 8 through 16 show the variation of ram-recovery ratio across the duct, with the propeller installed, for various inlet-velocity ratios, Mach numbers, and propeller blade angles. Figures 17 and 18 show the effect of advance-diameter ratio on the recoveries in the duct for several inlet-velocity ratios, Mach numbers, and propeller blade angles. Figures 19 through 22 show the effect of inlet-velocity ratio on the pressure recovery for several advance-diameter ratios and Mach numbers. Figure 23 shows a comparison of the ram-recovery ratios obtained as a function of inlet-velocity ratio with the propeller operating, ideal and platform junctures, and with the propeller removed.

DISCUSSION

A comparison of the recoveries obtained with the ideal juncture, the platform juncture, and with the propeller removed (fig. 23) shows that the addition of the propeller to the basic cowling-spinner combination resulted in an appreciable decrease in recovery due to thickening of the spinner boundary layer and other propeller interference effects. Little difference exists between the recoveries obtained for the two types of propeller-spinner junctures except for a blade angle of 40°. At this propeller blade angle, operation with the platform juncture resulted in increased recoveries over that for the ideal juncture.

The reason for the superior recoveries obtained with the platform-type juncture may be ascertained by a study of the recovery distributions presented in figures 8 to 16. It may be noted that at a blade angle of 40° (figs. 14, 15, and 16), higher recoveries were obtained near the inner surface of the duct with the platform juncture than were obtained with the ideal. This increase in recovery is believed to have resulted from either of the following conditions or from a combination of both: the spinner boundary layer becoming energized due to a vortex generated (reference 8) at the gap between the fixed and movable portions of the

propeller blade, or to this fixed portion being operated at a more
favorable angle than the equivalent propeller section for the ideal
juncture.

A further comparison of the recoveries presented in figure 23 shows
that, with the exception of the platform-type juncture with the propeller
blade angle of 40°, the recoveries with the propeller operating decreased
rapidly at inlet-velocity ratios below 0.8. At inlet-velocity ratios
above 0.8, the ram-recovery ratios were not affected by further increases
in inlet-velocity ratio. In the case of the platform juncture with
the propeller blade angle at 40°, recoveries remained relatively constant
at inlet-velocity ratios above 0.6. Below an inlet-velocity ratio
of 0.6, the recoveries decreased rapidly. Recoveries in excess of
90 percent were obtained (figs. 19 and 20) at inlet-velocity ratios
above 0.6 for propeller blade angles of 60° and 50°. For a propeller
blade angle of 40°, recoveries in excess of 90 percent were obtained at
inlet-velocity ratios above 0.7 for the ideal juncture and 0.5 for the
platform juncture. With the propeller removed, the recoveries decreased
rapidly at inlet-velocity ratios below 0.4 with recoveries greater than
96 percent being obtained at inlet-velocity ratios above 0.4 (fig. 23).

The effect of advance-diameter ratio and the effect of Mach number
(propeller operating) on the ram-recovery ratios was quite small
(figs. 17 to 22), resulting in minor increases in recovery with either
a decreasing advance-diameter ratio or a decreasing Mach number. The
largest change in recovery with advance-diameter ratio occurred for a
propeller blade angle of 40° due to the wider range of thrust coefficients
at which this blade angle was operated. With the propeller removed, no
appreciable effects of Mach number were apparent.

The data of reference 3, presenting the effect, at low Mach numbers,
of an eight-blade dual-rotation propeller operating ahead of the
NACA 1-62.8-070 D-cowl, show less effect of the operating propeller and
greater effect of advance-diameter ratio on the ram-recovery ratio
than do the data of this present investigation. This is believed to
be due to the difference in shape of the single and dual-rotation
spinners and to the differences arising from the operation of single
and dual-rotation propellers. However, the results showing a comparison
of the effects of the ideal and platform (with gap out of spinner bound-
ary layer) propeller-spinner junctures of reference 3 are similar to
those obtained with the two types of juncture used in this investigation.

There is a possibility that the recoveries obtained with the ideal
juncture might have been influenced by the abrupt change in thickness
ratio at about 15 percent of the propeller radius (figs. 3 and 4). It
is felt that higher recoveries might be obtained with a smoothly faired
extension of the propeller, in order to eliminate the possibility of
separation resulting from the oblique angle of air flow relative to the

discontinuity. In the case of the platform juncture, it is believed
that this same discontinuity in thickness would have no effect on the
pressure recoveries at propeller blade angles other than the design
condition.

<h2>CONCLUDING REMARKS</h2>

The following summarizing remarks can be made for the effects of
the propeller-spinner junctures on the pressure-recovery characteristics
of an NACA 1-series D-type cowl in combination with an NACA 1-series
spinner.

For the basic cowling-spinner combination with the propeller
removed, the ram-recovery ratio measured in the duct inlet was greater
than 0.96 at inlet-velocity ratios greater than 0.4 and was not affected
by compressibility within the range of Mach numbers covered in this
investigation. At inlet-velocity ratios less than 0.4, boundary-layer
build up over the spinner caused large losses in recovery at the inner
surface of the duct.

Little difference was obtained in the ram-recovery ratios for the
ideal and platform junctures, except for a propeller blade angle of 40°
where the platform juncture was superior to the ideal juncture.

The addition of an operating propeller to the basic cowling-spinner
combination resulted in a decrease in pressure recovery and required an
increase in the inlet-velocity ratio in order to avoid excessive losses
in the duct.

With the propeller operating ahead of the inlet, the ram-recovery
ratio increased with increasing inlet-velocity ratio up to an inlet-
velocity ratio of 0.8, except for the platform juncture with the
40° propeller blade angle. Above this value, inlet-velocity ratio had
little or no effect on the ram-recovery ratio. For the platform juncture
with the propeller blade angle at 40°, the pressure recoveries were rela-
tively constant above an inlet-velocity ratio of 0.6. Below an inlet-
velocity ratio of 0.6, the recoveries decreased rapidly.

The effect of advance-diameter ratio and the effect of Mach number
(propeller operating) on the pressure recoveries was quite small.

Ames Aeronautical Laboratory,
    National Advisory Committee for Aeronautics
        Moffett Field, Calif.

REFERENCES

1. Hanson, Frederick H., Jr., and Mossman, Emmet A.: Effect of Pressure
   Recovery on the Performance of a Jet-Propelled Airplane.
   NACA TN 1695, 1948.

2. Nichols, Mark R., and Keith, Arvid L., Jr.: Investigation of a
   Systematic Group of NACA 1-Series Cowlings with and without
   Spinners. NACA Rep. 950, 1949. (Formerly NACA RM L8A15)

3. Keith, Arvid L., Jr., Bingham, Gene J., and Rubin, Arnold J.:
   Effects of Propeller-Shank Geometry and Propeller-Spinner-Juncture
   Configuration on Characteristics of an NACA 1-Series Cowling-
   Spinner Combination With an Eight-Blade Dual-Rotation Propeller.
   NACA RM L51F26, 1951.

4. Crigler, John L., and Talkin, Herbert W.: Propeller Selection from
   Aerodynamic Considerations. NACA ACR, July 1942.

5. Uddenberg, R. C.: Characteristics and Design of Shielded Total-Head
   Tubes. Rep. D-4265, Boeing Aircraft Co., Aug. 19, 1942.

6. Smith, Norman F.: Numerical Evaluation of Mass-Flow Coefficient
   and Associated Parameters from Wake Survey Equations.
   NACA TN 1381, 1947.

7. Herriot, John G.: Blockage Corrections for Three-Dimensional-Flow
   Closed-Throat Wind Tunnels, with Consideration of the Effect of
   Compressibility. NACA Rep. 995, 1950. (Formerly NACA RM A7B28)

8. Taylor, H. D.: Summary Report on Vortex Generators. U.A.C.
   Rep. R-05280-9, United Aircraft Corp., Res. Dept., Mar. 7, 1950.

TABLE I.- COWLING-SPINNER COORDINATES

[Coordinates in inches]

x_s/X_s x_c/X_c x_1/X_1	Distance from leading edge of spinner (x_s)	NACA 1-46.5-047 spinner, radius (r_s)	Distance from leading edge of cowl (x_c)	NACA 1-62.8-070 cowl, radius (r_c)	Distance from leading edge of cowl (x_1)	NACA 1-series inner lip, radius (r_1)
0	0	0	0	4.460	0	4.460
.2	.013	.156	.020	4.581	-----	-----
.4	.026	.216	.039	4.628	-----	-----
.6	.039	.264	.059	4.666	-----	-----
.8	.053	.304	.078	4.697	-----	-----
1.0	.066	.338	.098	4.723	-----	-----
1.5	.099	.414	.147	4.783	-----	-----
2.0	.132	.479	.196	4.834	.008	4.439
3.0	.197	.596	.294	4.925	-----	-----
4.0	.263	.699	.392	5.005	.017	4.429
5.0	.329	.793	.490	5.078	-----	-----
6.0	.395	.879	.588	5.146	-----	-----
8.0	.526	1.035	.784	5.268	.034	4.415
10.0	.658	1.176	.980	5.377	-----	-----
12.0	.790	1.305	1.176	5.478	.050	4.403
14.0	.921	1.421	1.372	5.569	-----	-----
16.0	1.053	1.526	1.568	5.651	.067	4.394
18.0	1.184	1.624	1.764	5.727	-----	-----
20.0	1.316	1.715	1.960	5.798	.084	4.386
22.0	1.448	1.802	2.156	5.866	-----	-----
24.0	1.579	1.885	2.352	5.931	.101	4.378
26.0	1.711	1.964	2.548	5.993	-----	-----
28.0	1.842	2.040	2.744	6.052	.118	4.372
30.0	1.974	2.112	2.940	6.108	-----	-----
32.0	2.106	2.182	3.136	6.162	.134	4.366
34.0	2.237	2.249	3.332	6.215	-----	-----
36.0	2.369	2.313	3.528	6.265	-----	-----
38.0	2.500	2.374	3.724	6.313	-----	-----
40.0	2.632	2.433	3.920	6.359	.168	4.355
42.0	2.764	2.489	4.116	6.403	-----	-----
44.0	2.895	2.544	4.312	6.445	-----	-----
46.0	3.027	2.596	4.508	6.485	-----	-----
48.0	3.158	2.645	4.704	6.524	.202	4.346
50.0	3.290	2.692	4.900	6.560	-----	-----
54.0	3.553	2.781	5.292	6.630	.244	4.337
58.0	3.816	2.863	5.684	6.694	-----	-----
62.0	4.080	2.938	6.076	6.751	.277	4.331
66.0	4.343	3.001	6.468	6.802	-----	-----
70.0	4.606	3.058	6.860	6.846	.311	4.326
74.0	4.869	3.108	7.252	6.885	-----	-----
78.0	5.132	3.151	7.644	6.918	.344	4.323
82.0	5.396	3.186	8.036	6.946	-----	-----
86.0	5.659	3.214	8.428	6.968	-----	-----
90.0	5.922	3.235	8.820	6.985	.378	4.320
94.0	6.185	3.250	9.212	6.996	-----	-----
98.0	6.448	3.254	9.604	6.999	-----	-----
100.0	6.580	3.255	9.800	7.000	.420	4.320
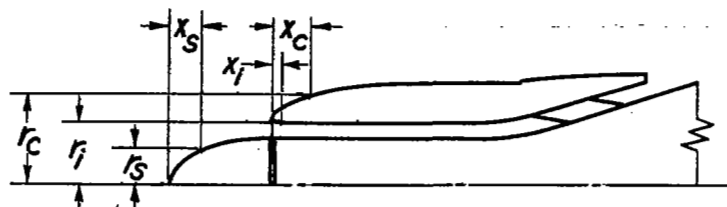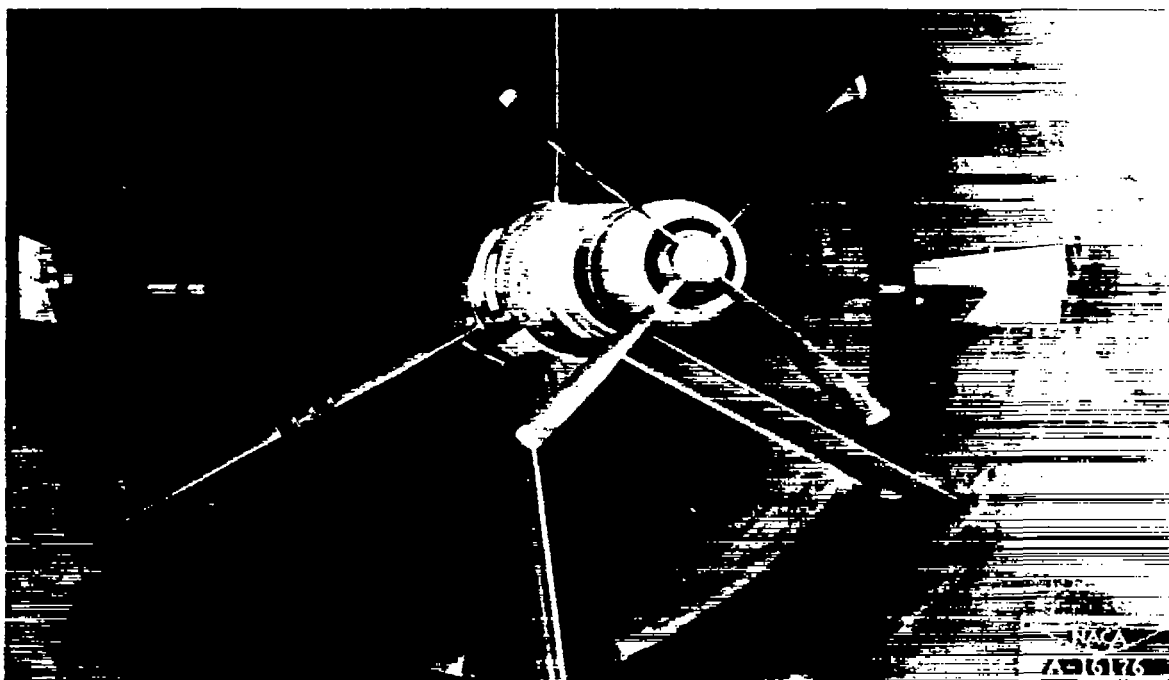
Figure 1.— The model mounted on the 1000-horsepower dynamometer in the 12-foot pressure wind tunnel.

NACA 4-(5)(05)-041
Single rotation propeller
(developed plan form)

Note: Dimensions shown in inches.

NACA 16-series sections

24.00

6.58

4.18

9.80

NACA 1-62.8-070 Cowl

Platform juncture

2.80

7.00

Sliding throttle

0.025

3.60

1/32

3.26

4.32

Model center line

NACA 1-46.5-047 Spinner

Sta. ① (Ram-recovery rake location)
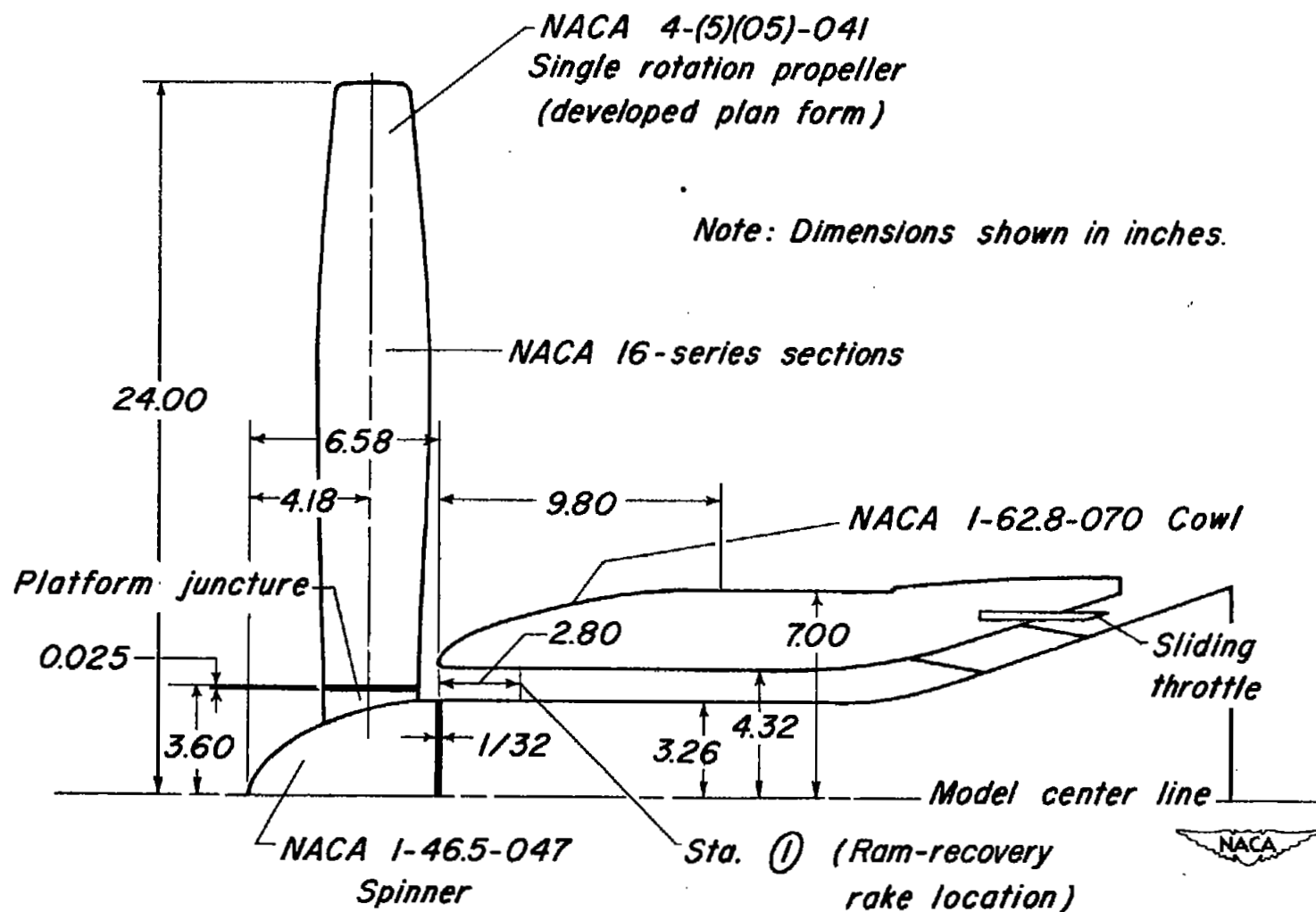
Figure 2. – Model arrangement.
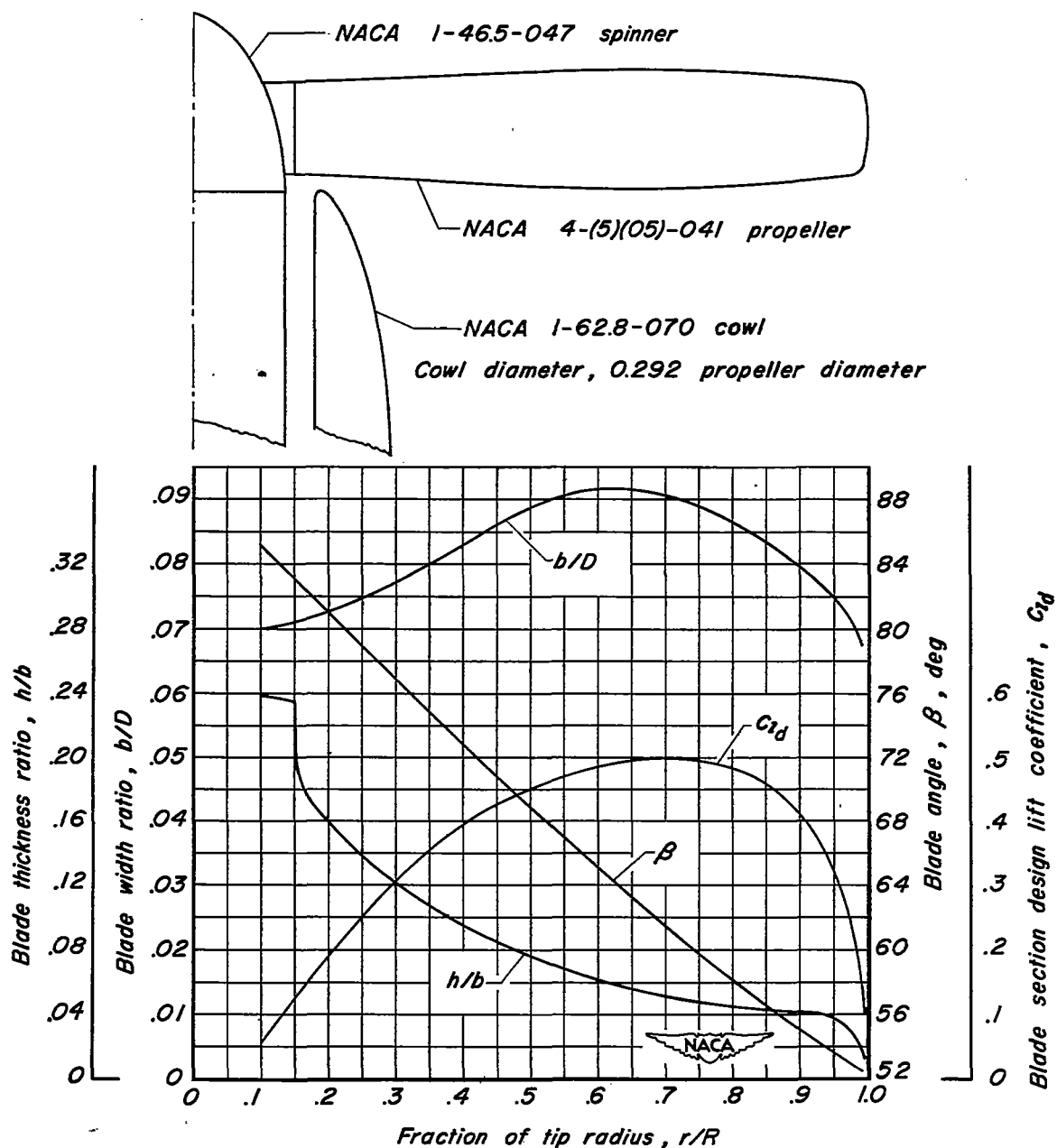
Figure 3.- Plan-form and blade-form curves for the NACA 4-(5)(05)-041 four-blade propeller.
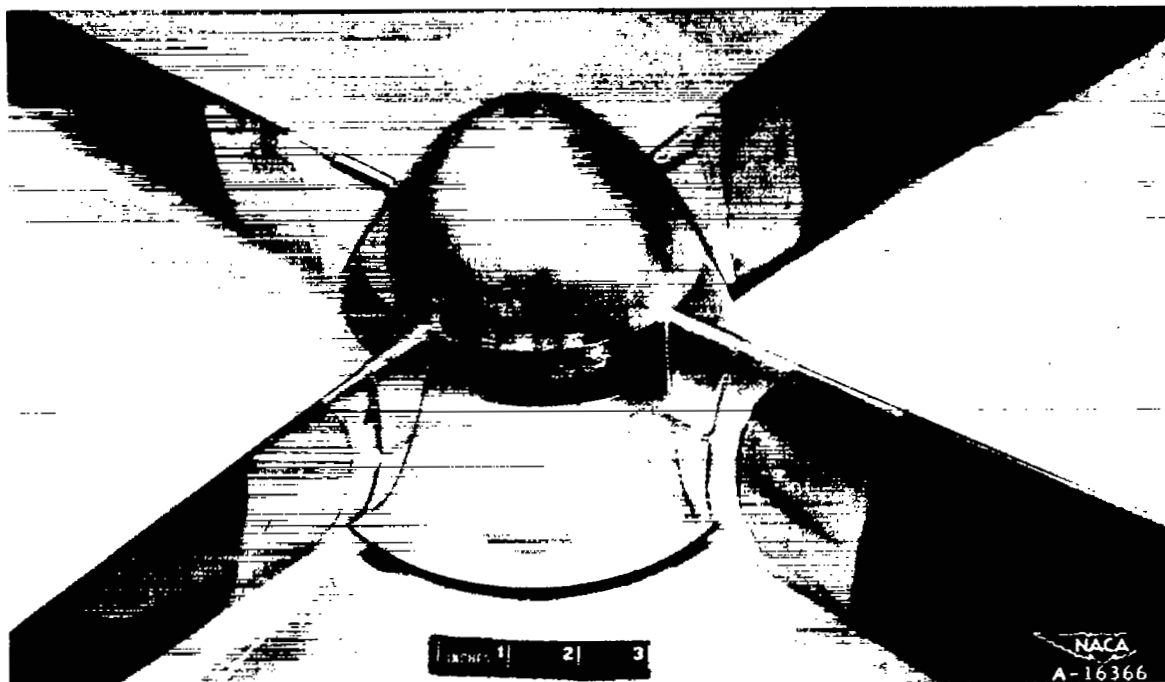
Figure 4.— Ideal propeller—spinner juncture; β, 60°.
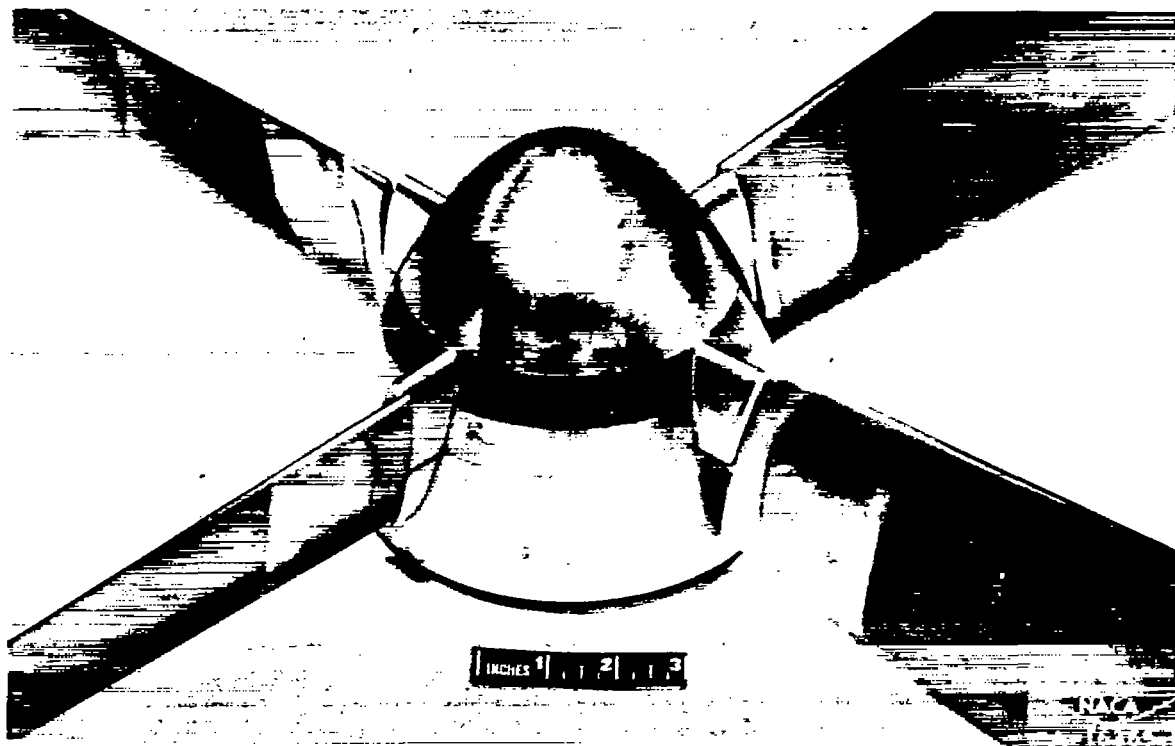
Figure 5.— Platform propeller—spinner juncture; β, 50°.

Figure 6.— Close—up of the model showing pressure—rake locations.
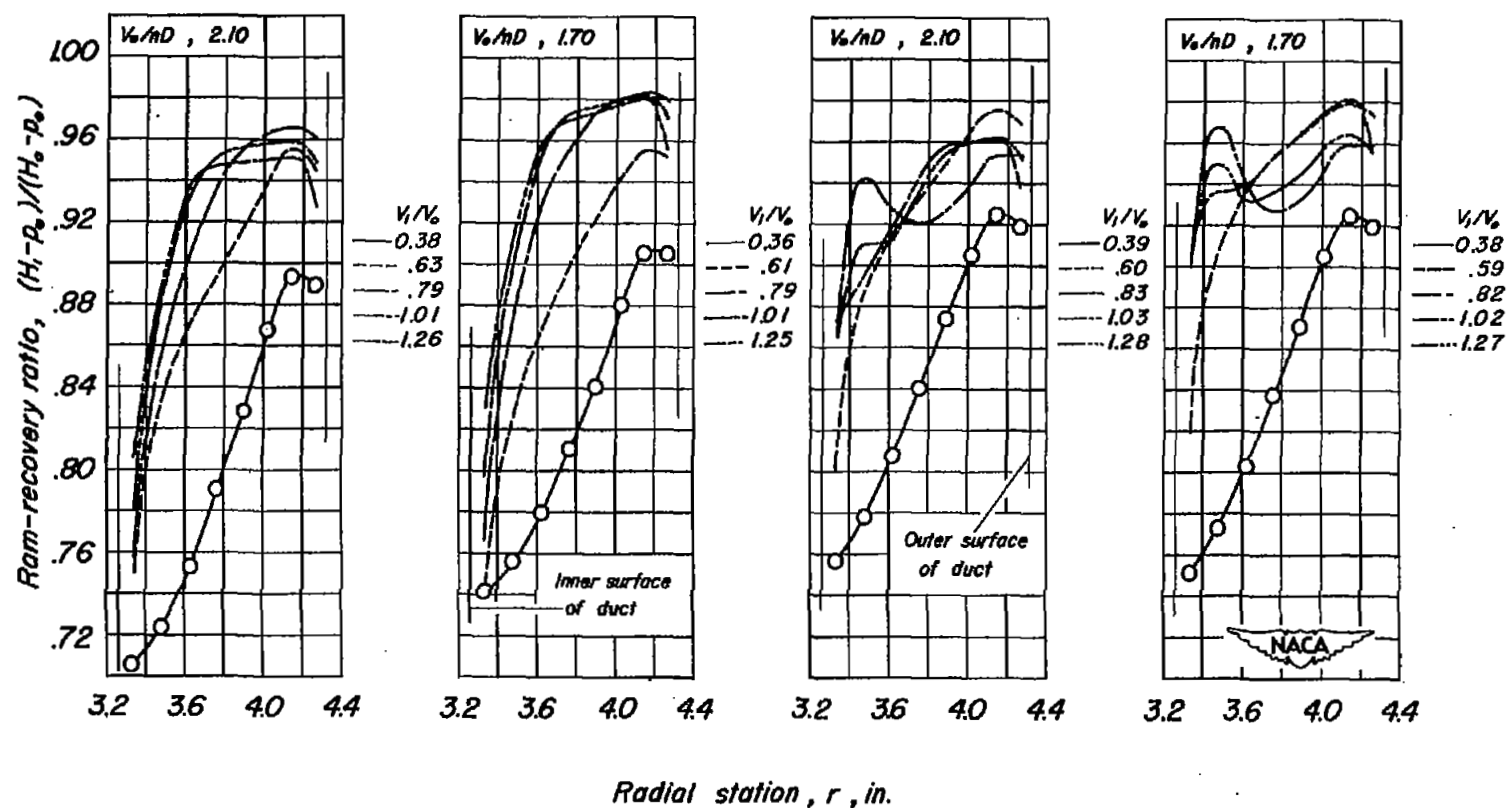
(a) M_o, 0.83   (b) M_o, 0.79   (c) M_o, 0.69   (d) M_o, 0.59
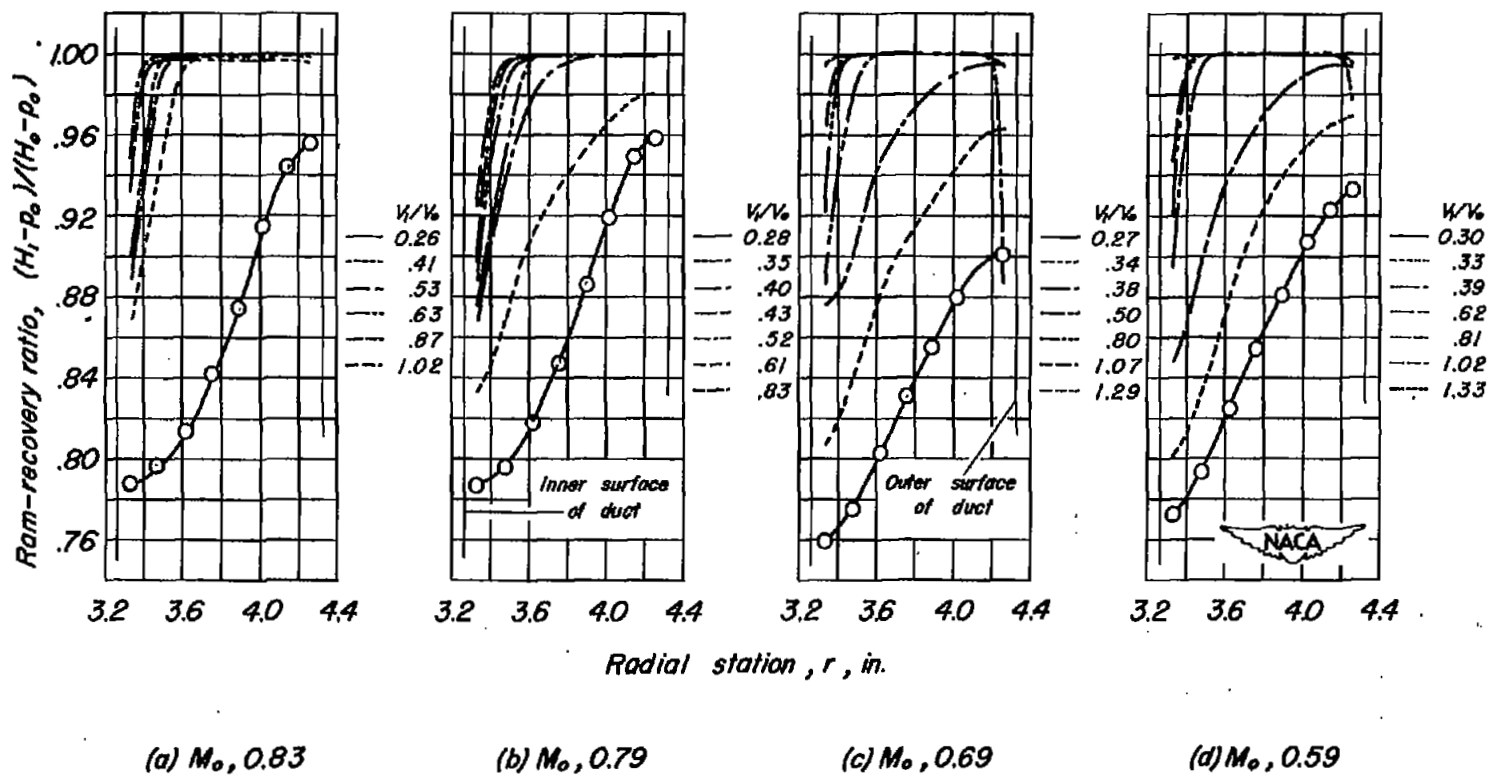
Figure 7.—The variation of the average ram-recovery ratio with radial station across the duct for various inlet-velocity ratios, propeller removed.
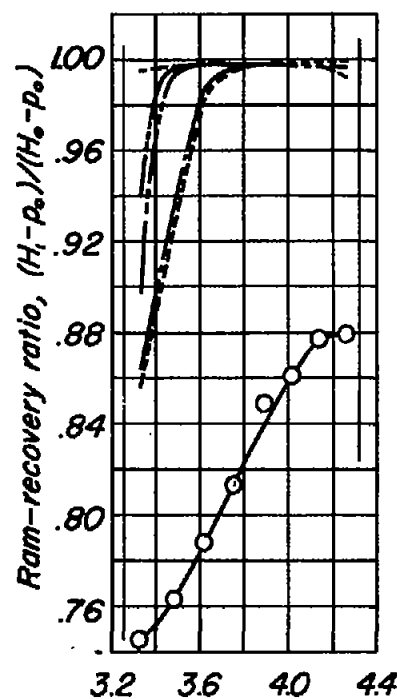
(e) M_o, 0.39
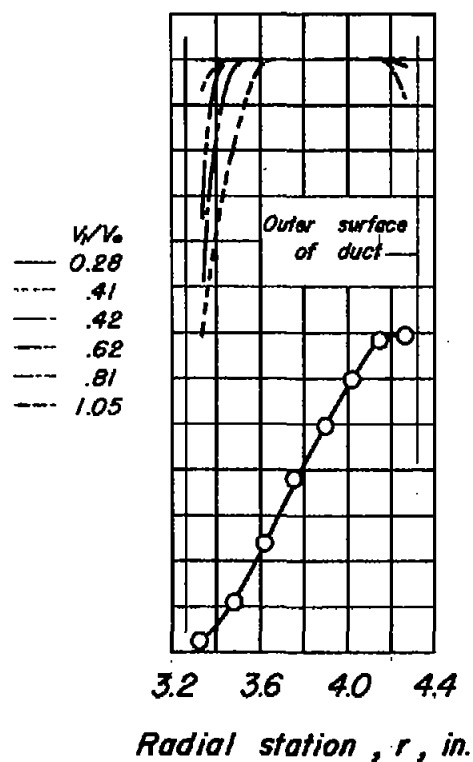
(f) M_o, 0.30
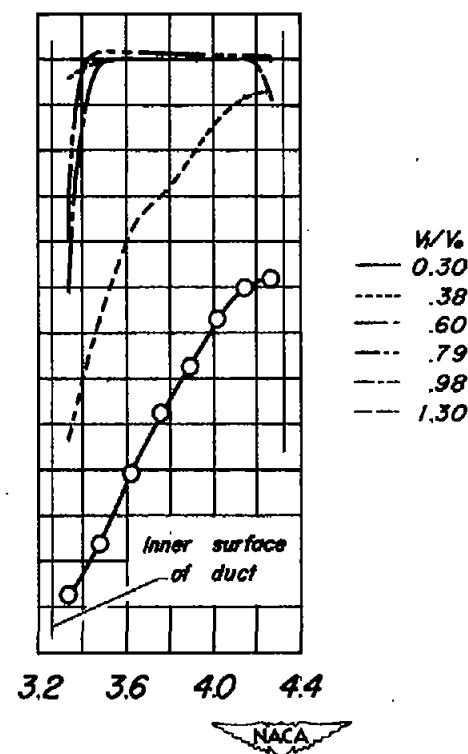
(g) M_o, 0.20

Figure 7.- Concluded.
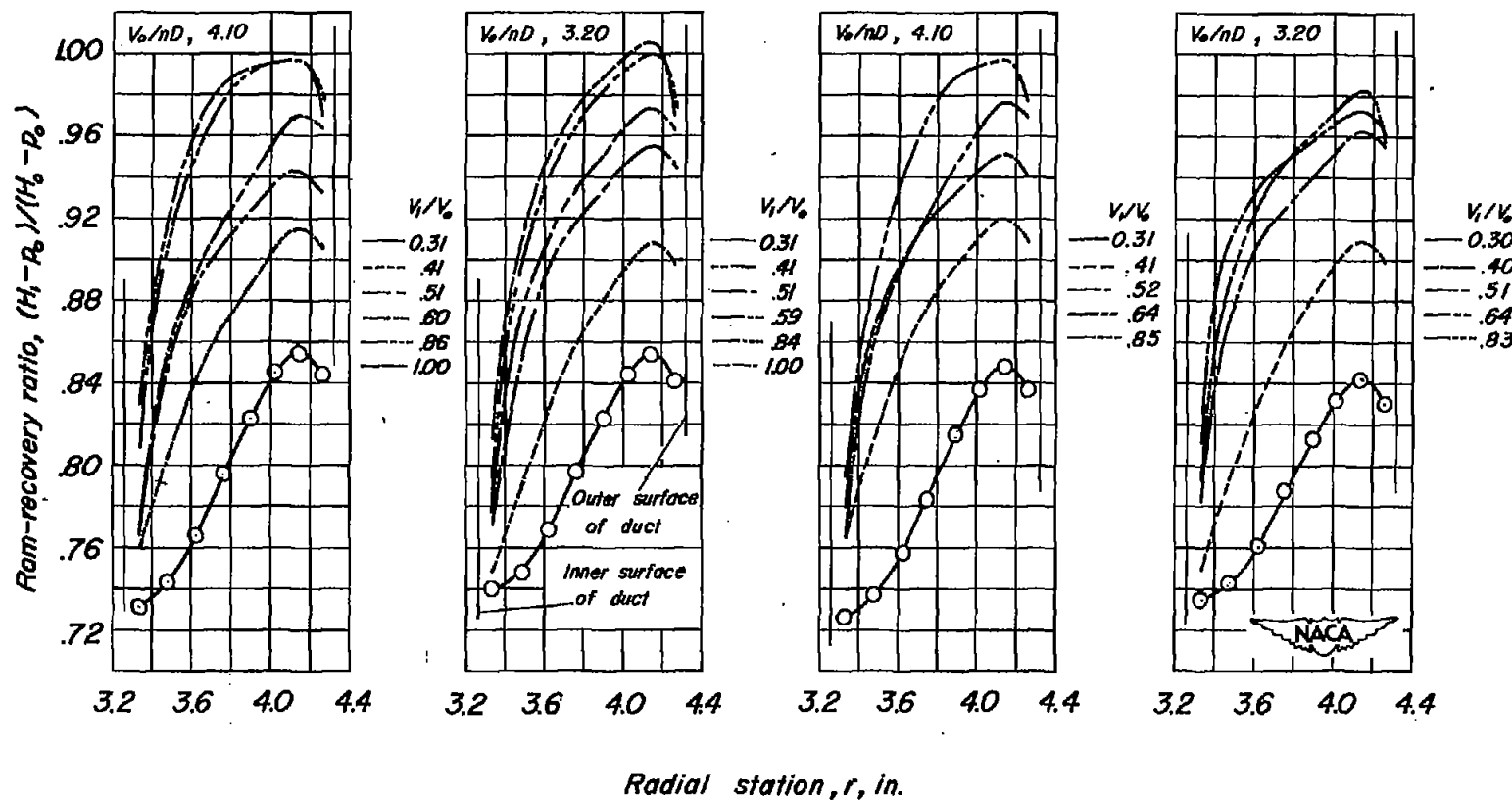
(a) Ideal junctures.　　　　　*(b) Platform junctures.*

Figure 8.—The variation of the average ram-recovery ratio with radial station across the duct for various inlet-velocity ratios ; M_o, 0.83; β, 60°.
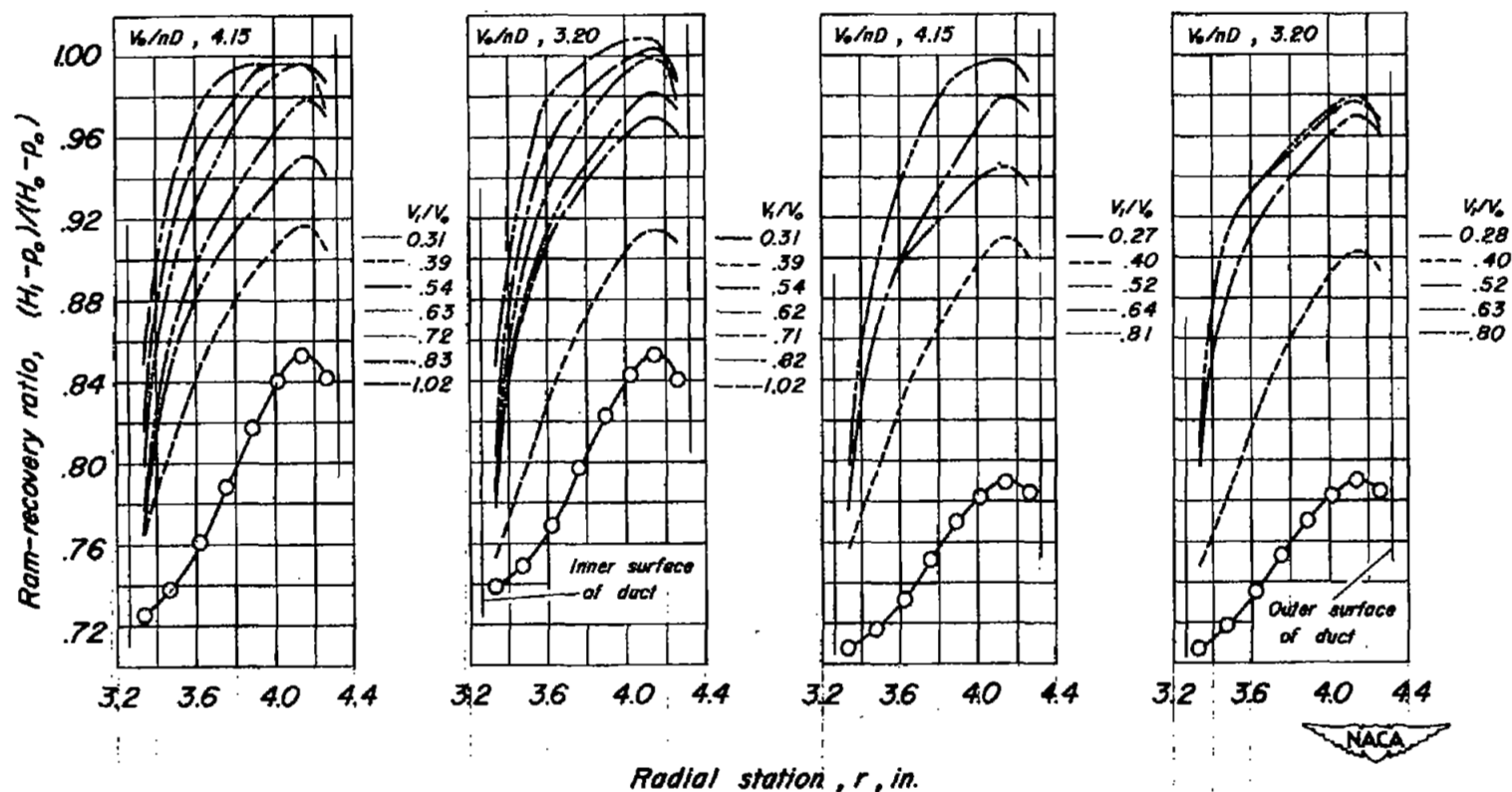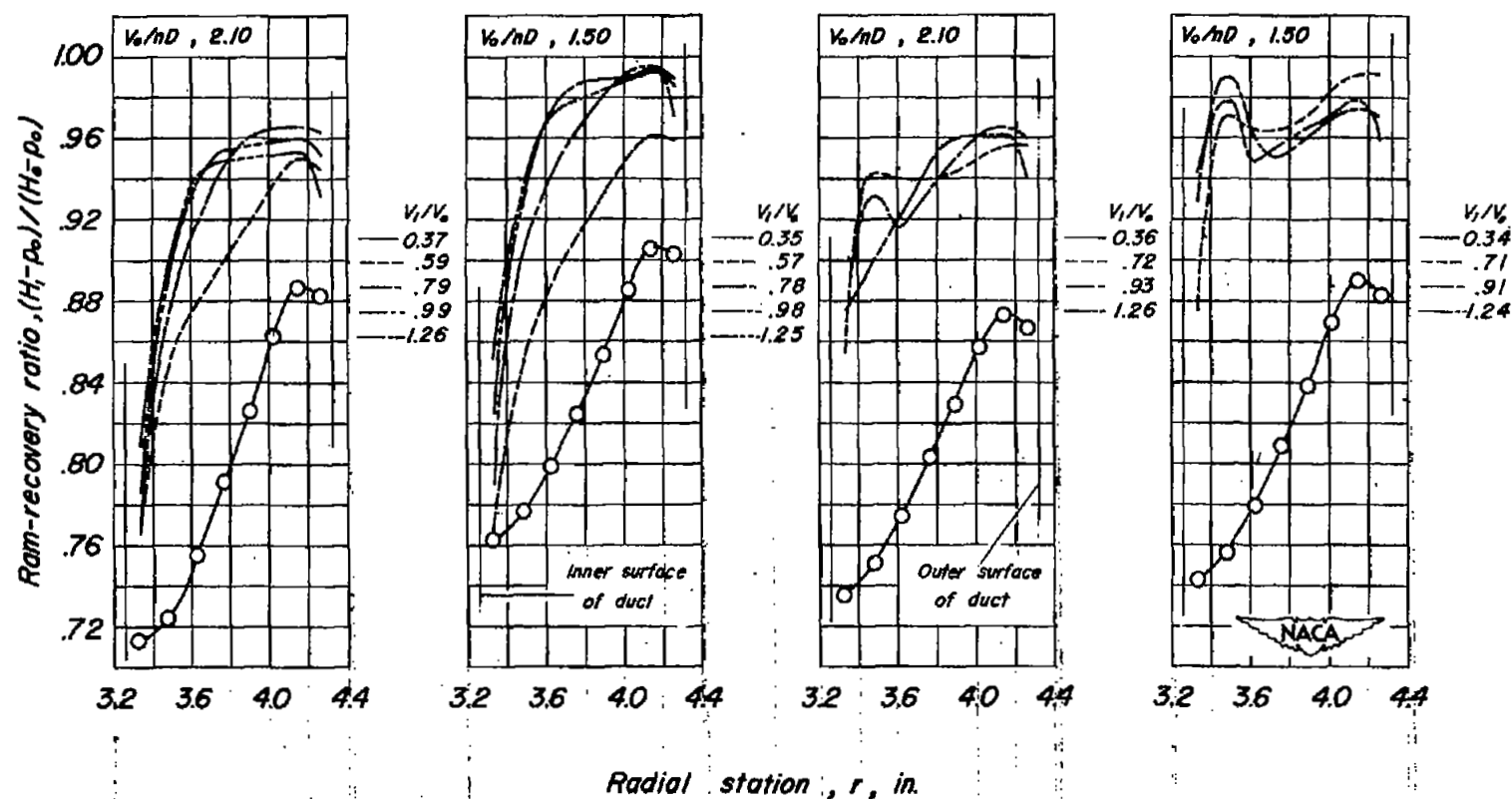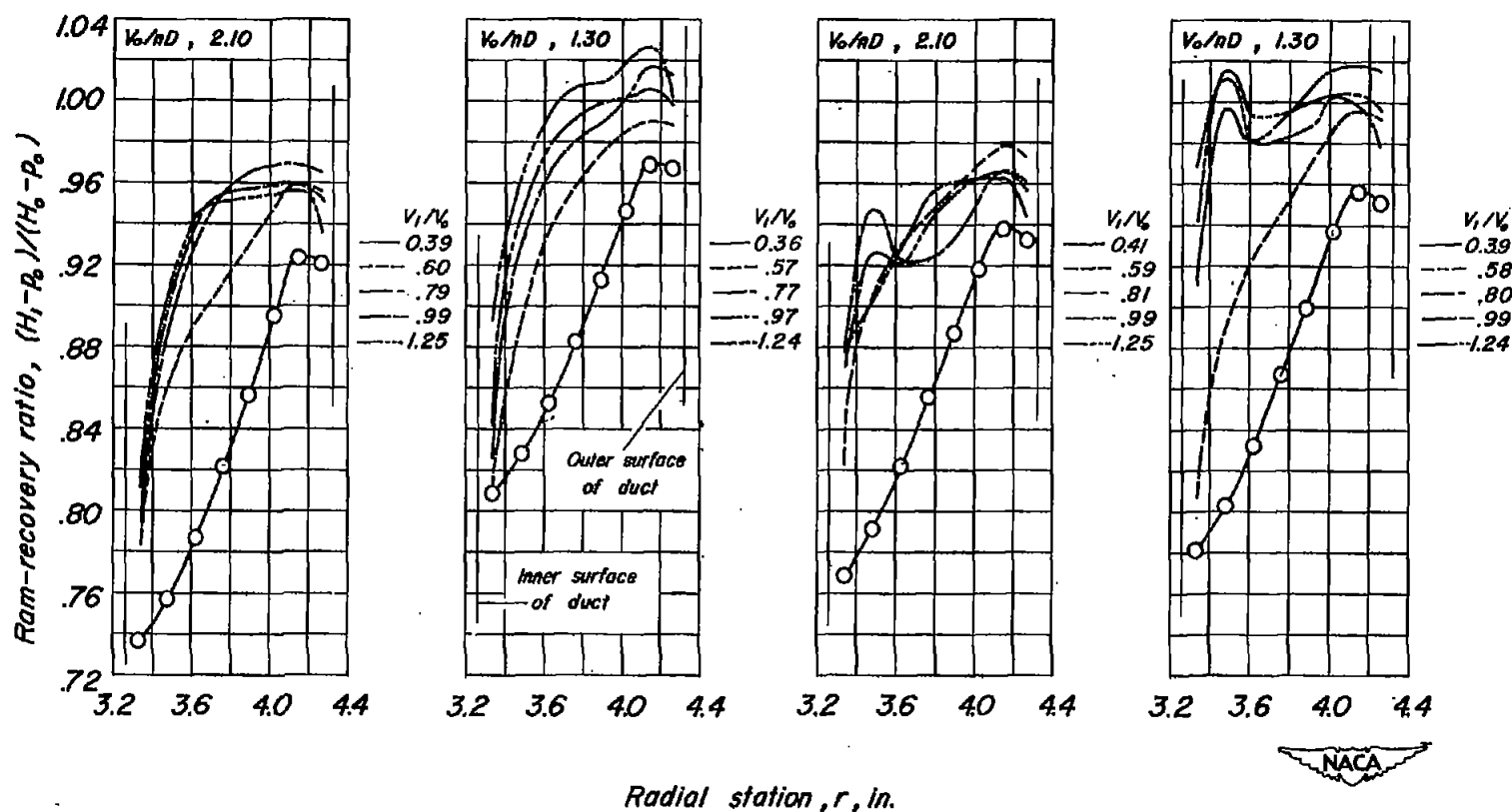
(a) Ideal junctures.

(b) Platform junctures.

Figure 9.—The variation of the average ram-recovery ratio with radial station across the duct for various inlet-velocity ratios; M_o, 0.79; β, 60°.
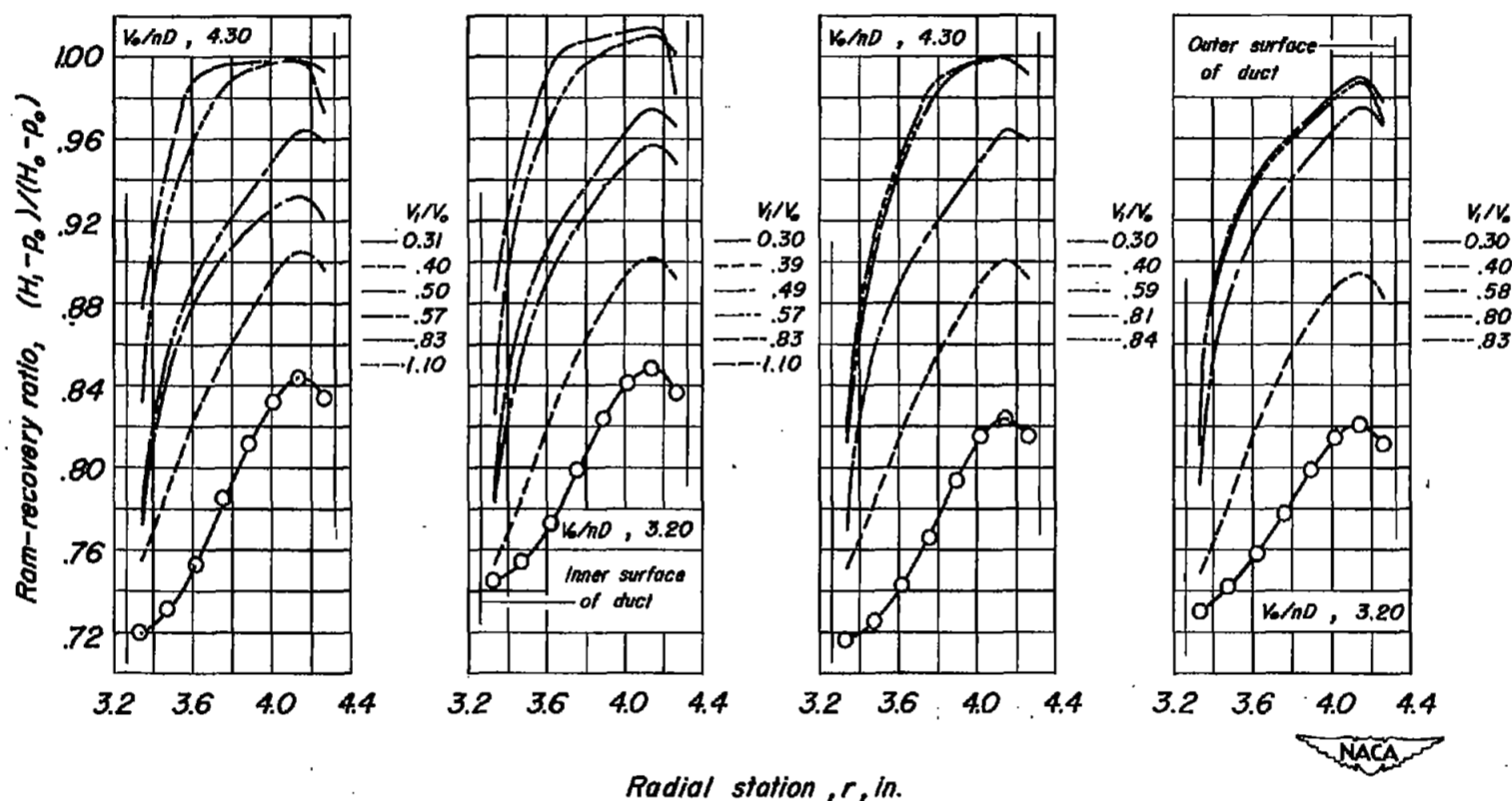
(a) Ideal junctures.

(b) Platform junctures.

Figure 10.—The variation of the average ram-recovery ratio with radial station across the duct for various inlet-velocity ratios ; M_o, 0.69; β, 60°.
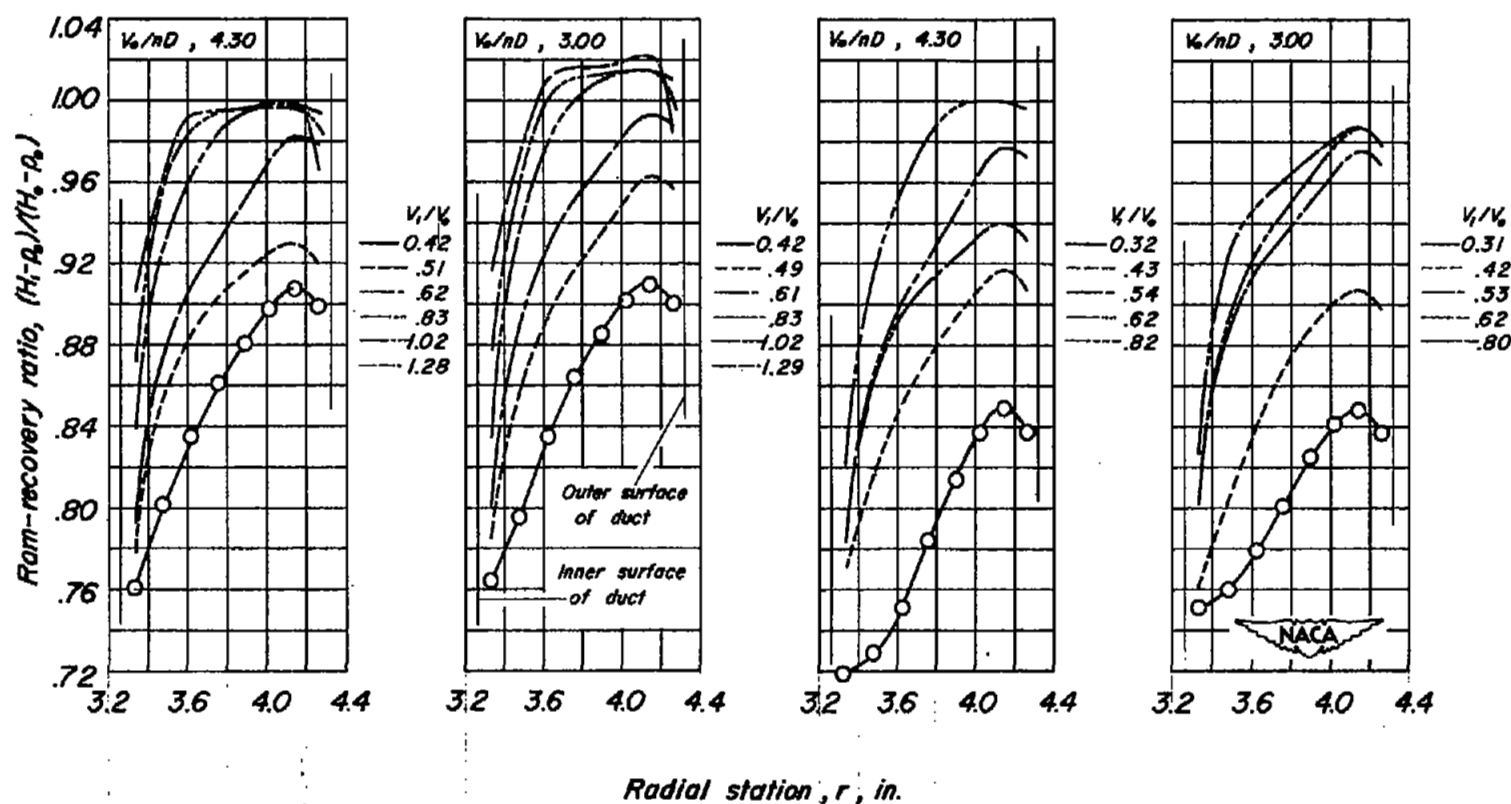
(a) Ideal junctures.

(b) Platform junctures.

Figure II.— The variation of the average ram-recovery ratio with radial station across the duct for various inlet-velocity ratios; M_o, 0.59; β, 60°.
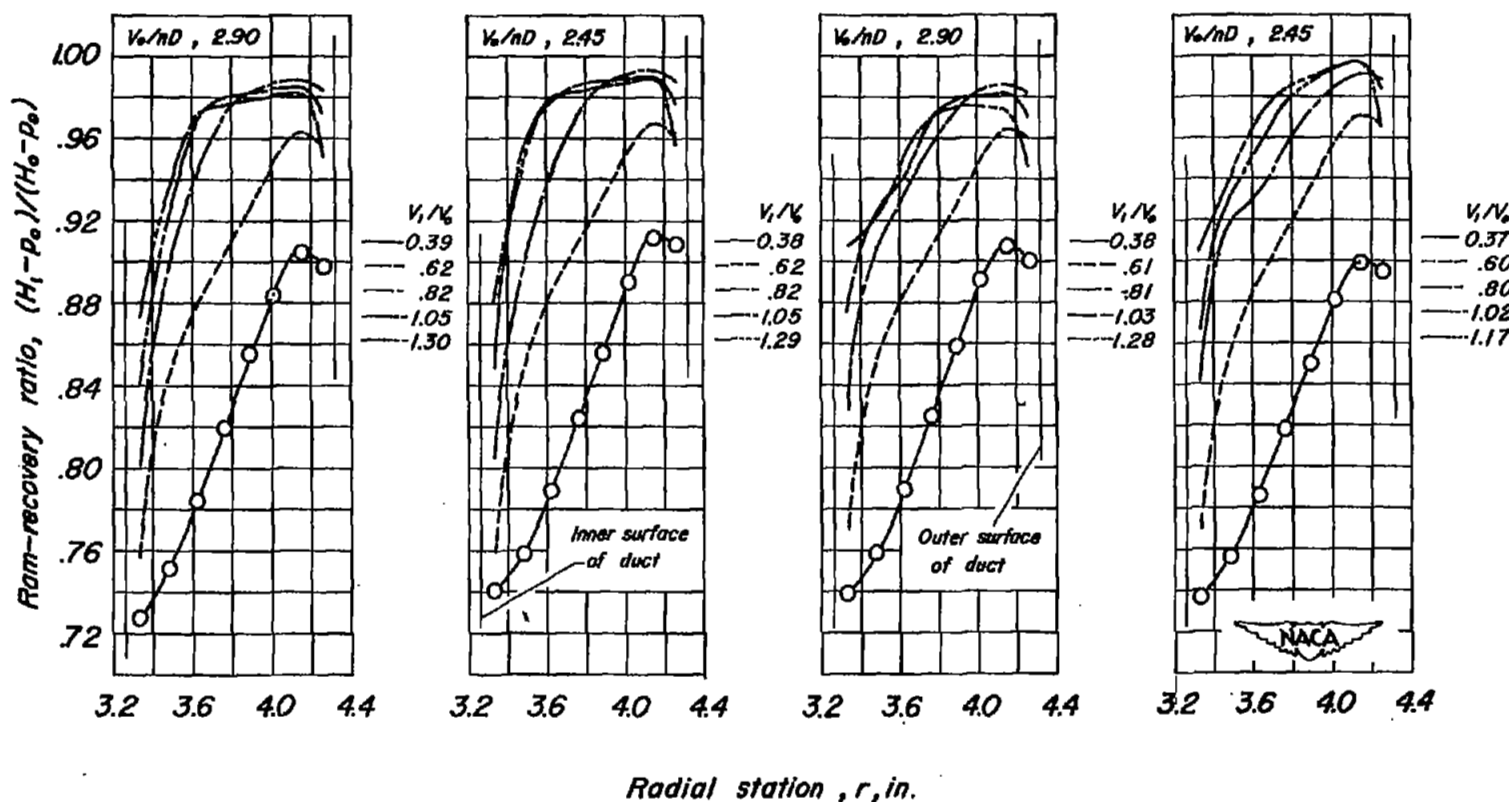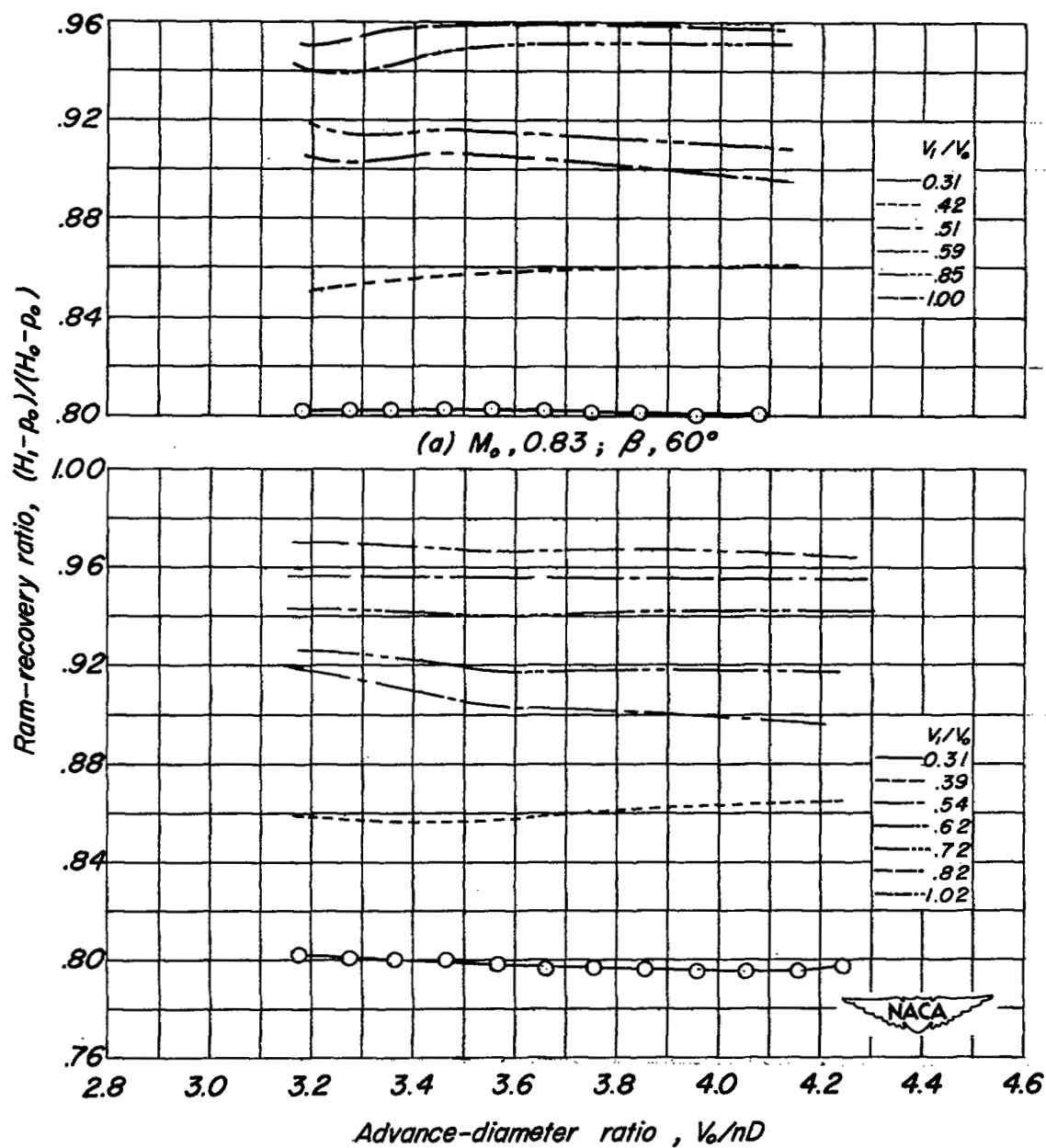
(a) Ideal junctures.

(b) Platform junctures.

Figure 12.-The variation of the average ram-recovery ratio with radial station across the duct for various inlet-velocity ratios; M_o, 0.59; β, 50°.
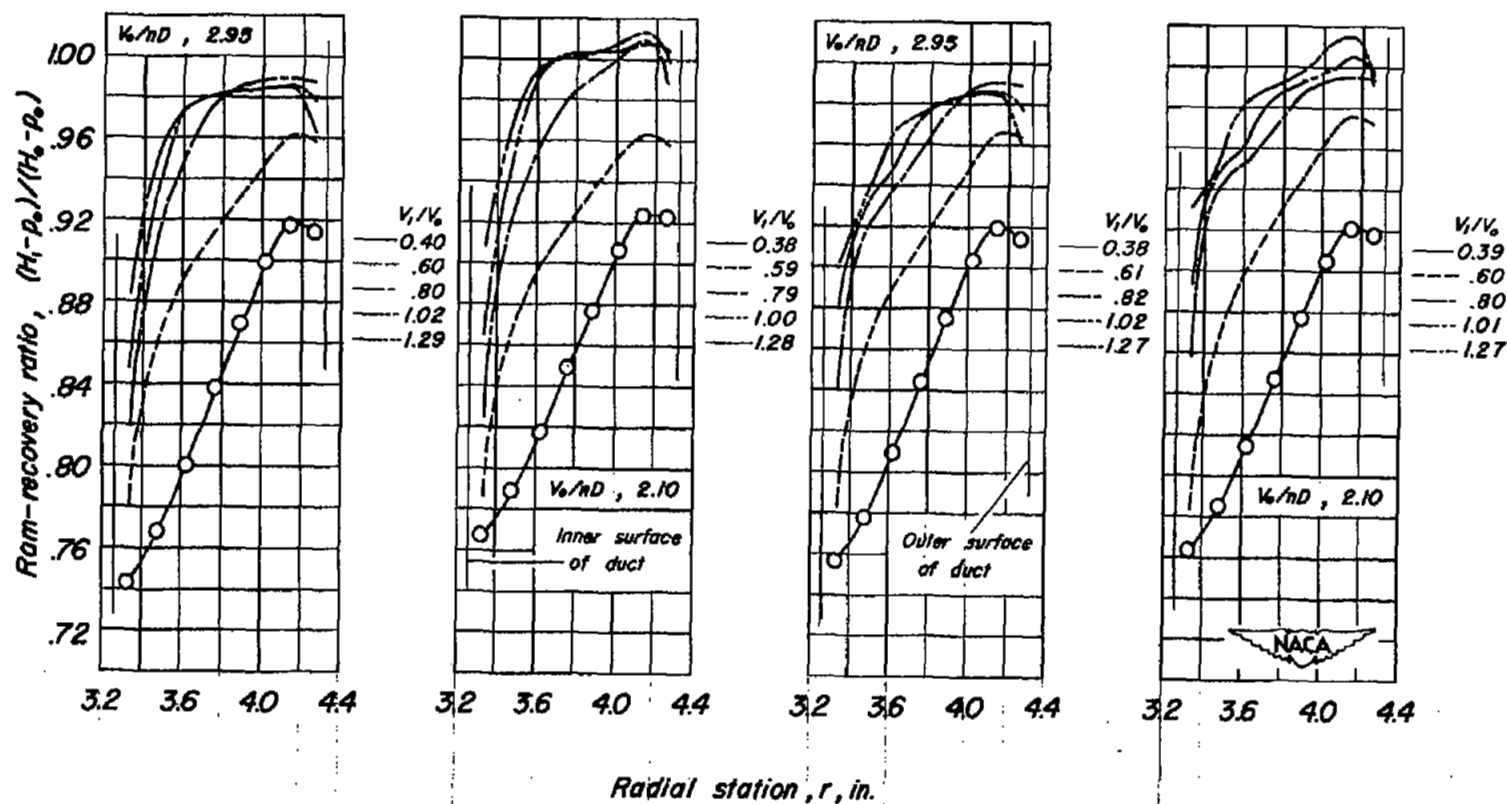
(a) Ideal junctures.

(b) Platform junctures.

Figure 13.-The variation of the average ram-recovery ratio with radial station across the duct for various inlet-velocity ratios ; M_0, 0.39; β, 50°.

(a) Ideal junctures.　　　　　　(b) Platform junctures.

Figure 14.—The variation of the average ram-recovery ratio with radial station across the duct for various inlet-velocity ratios ;　M_o, 0.39; β, 40°.

Figure 15.-The variation of the average ram-recovery ratio with radial station across the duct for various inlet-velocity ratios; M_o, 0.30; β, 40°.

(a) Ideal junctures.

(b) Platform junctures.

Figure 16.—The variation of the average ram-recovery ratio with radial station across the duct for various inlet-velocity ratios ; M_o, 0.20; β, 40°.

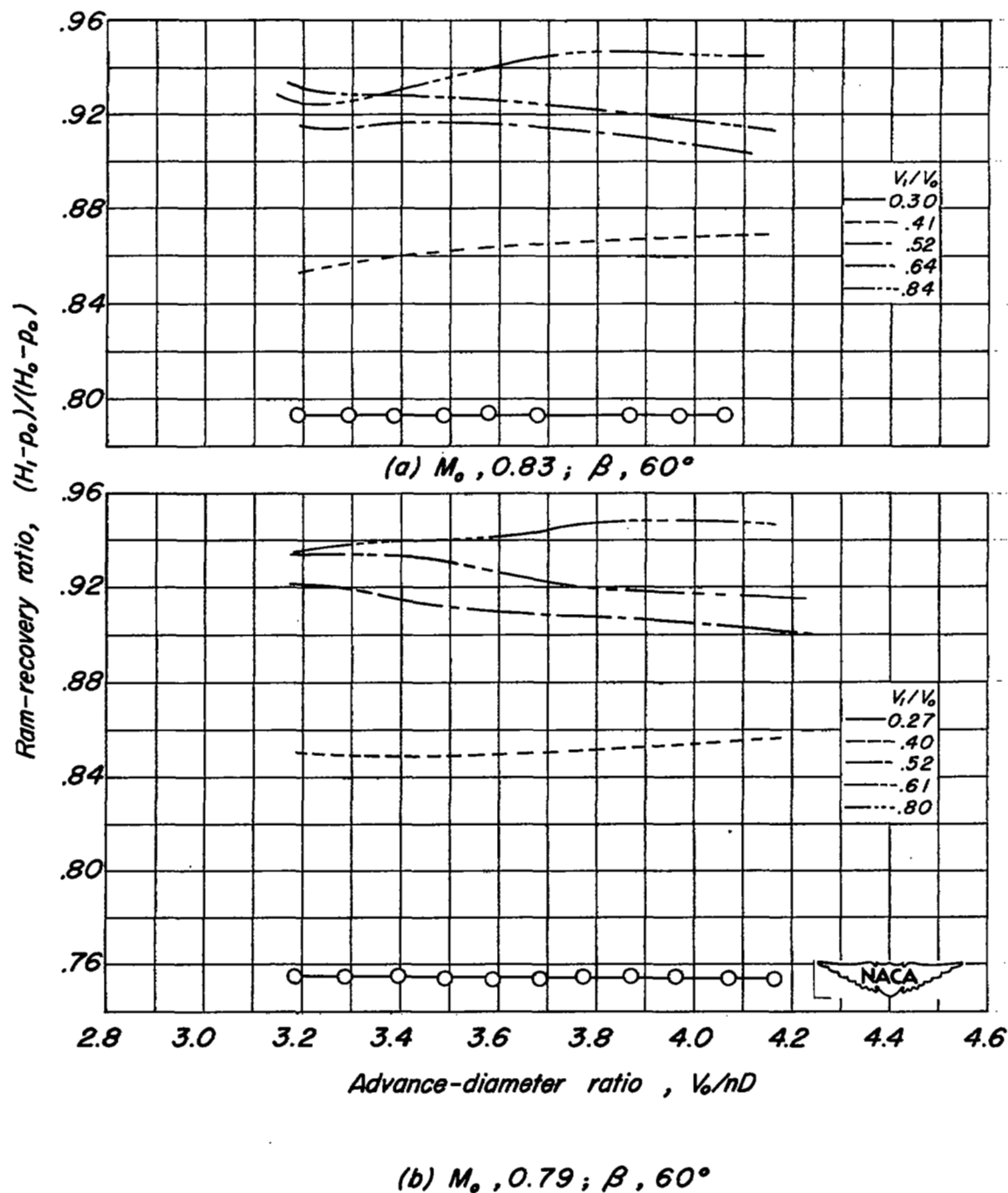(a) M_o, 0.83 ; β, 60°

(b) M_o, 0.79; β, 60°

Figure 17.— The variation of the average ram-recovery ratio with advance-diameter ratio for various inlet-velocity ratios, ideal junctures.
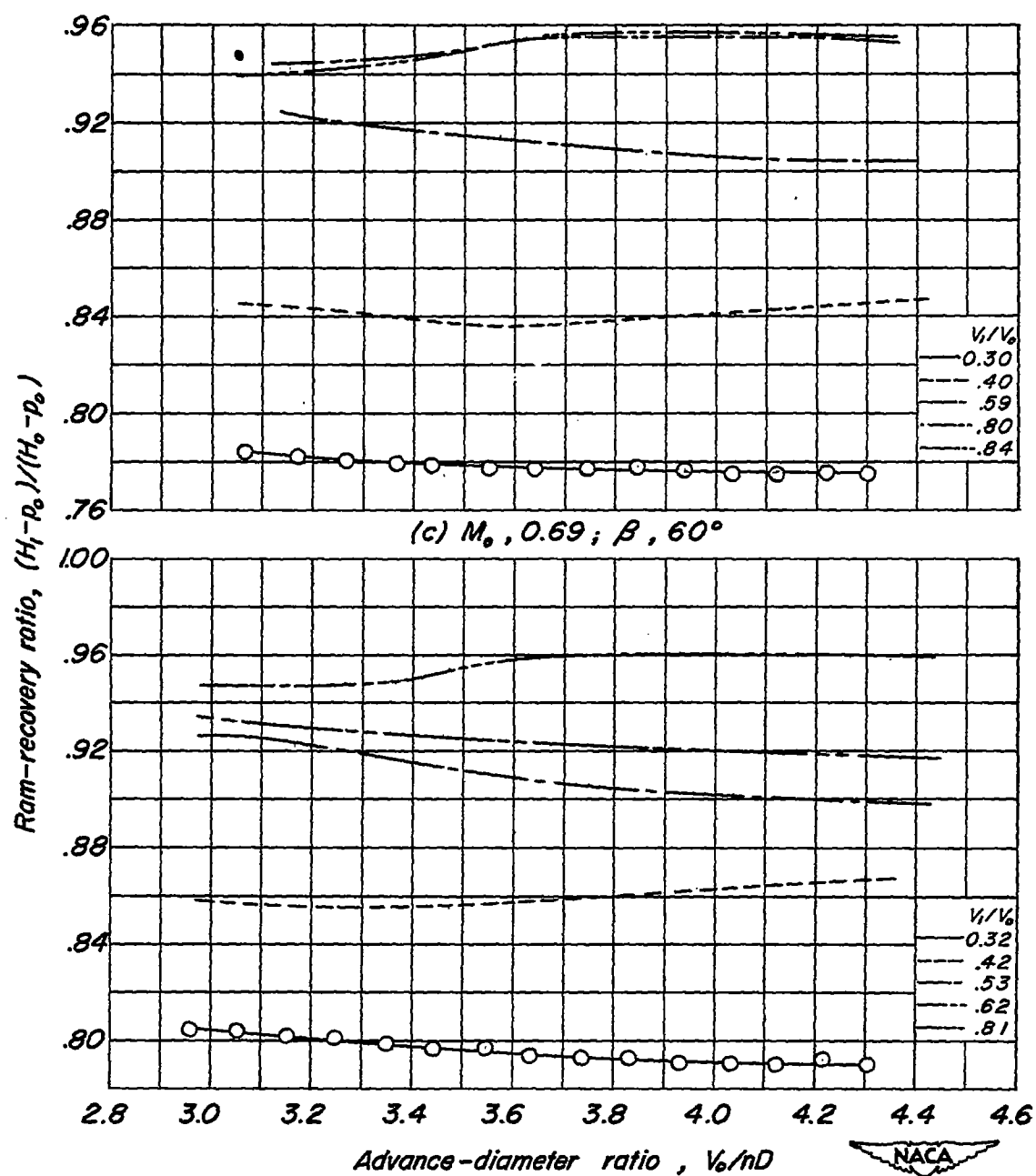
(c) M_o, 0.69; β, 60°
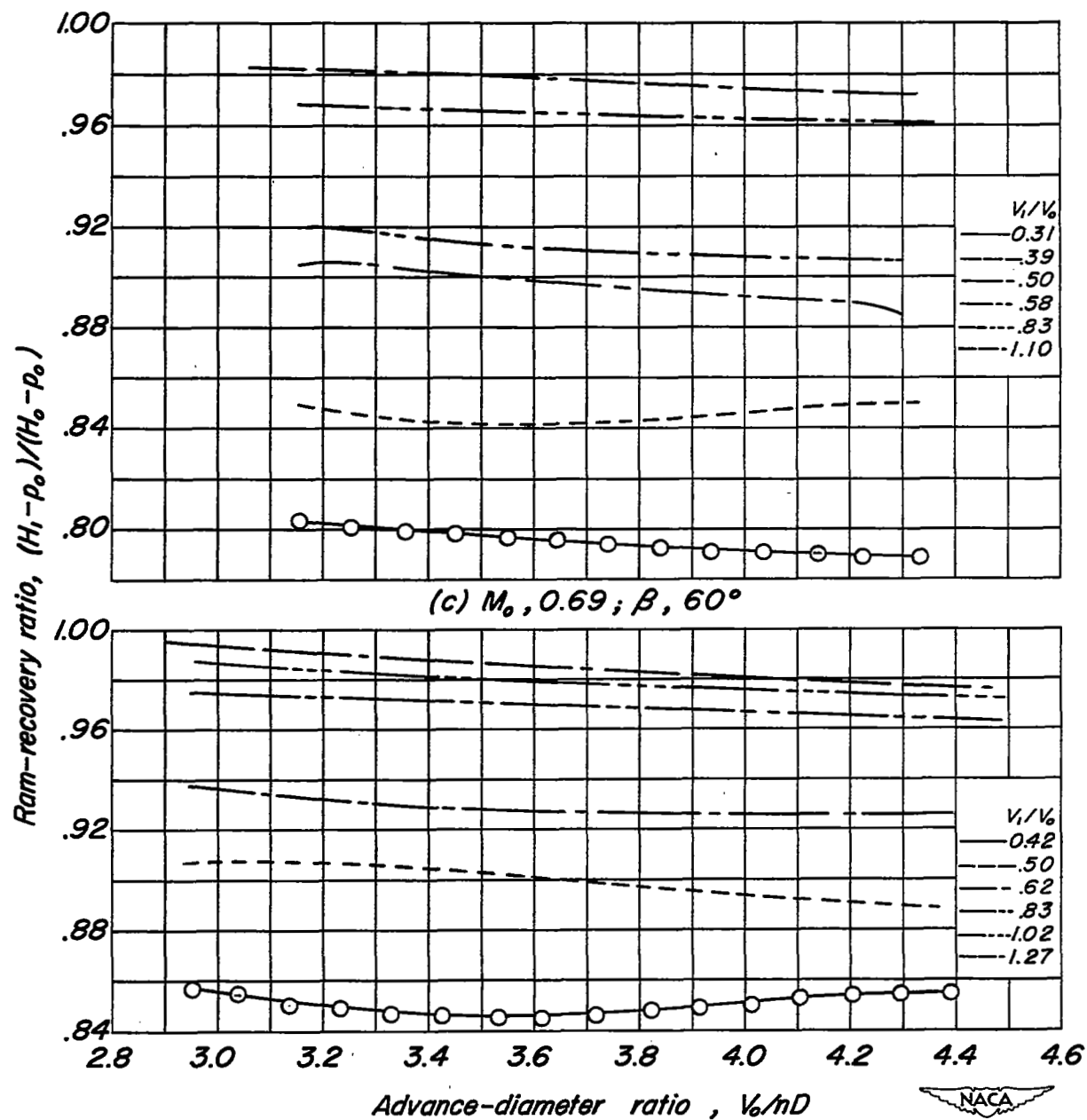
(d) M_o, 0.59; β, 60°

Figure 17.—Continued.

(e) M_o, 0.59; β, 50°
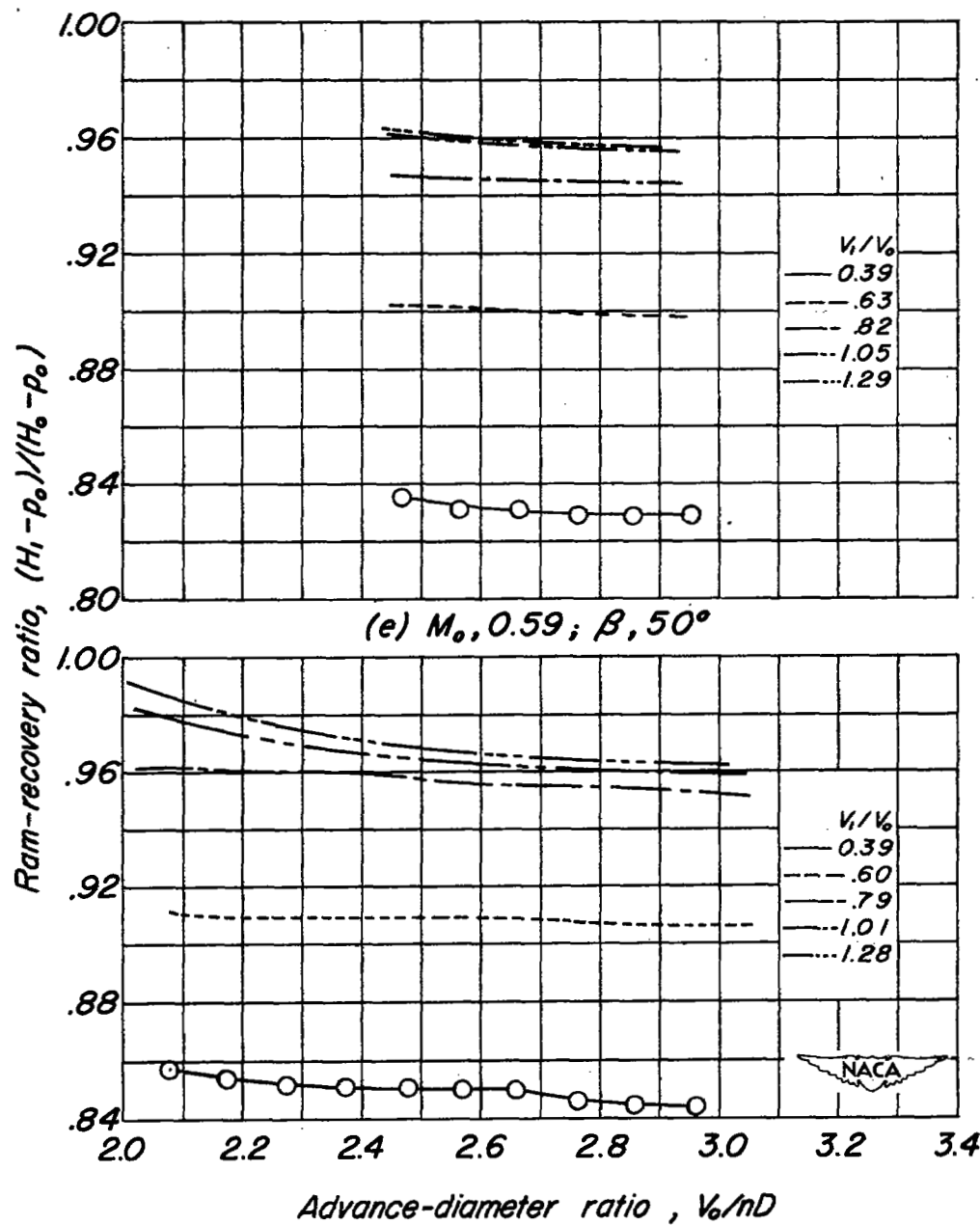
(f) M_o, 0.39; β, 50°

Figure 17.— Continued.
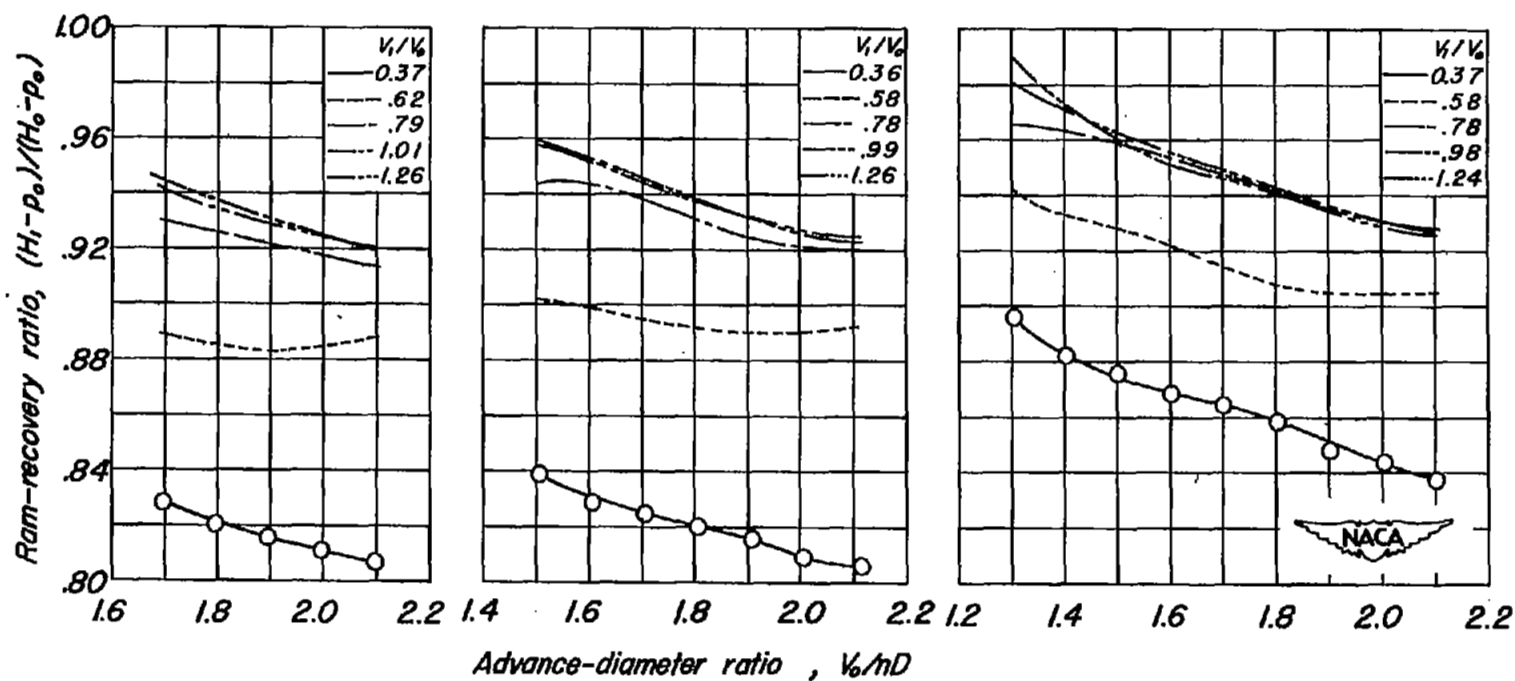
(g) M_o, 0.39; β, 40°   (h) M_o, 0.30; β, 40°   (i) M_o, 0.20; β, 40°

Figure 17.- Concluded.

(a) M_o , 0.83 ; β , 60°

(b) M_o , 0.79 ; β , 60°

Figure 18.—The variation of the average ram-recovery ratio with advance-diameter ratio for various inlet-velocity ratios, platform junctures.

(c) M_o , 0.69 ; β , 60°

(d) M_o , 0.59 ; β , 60°
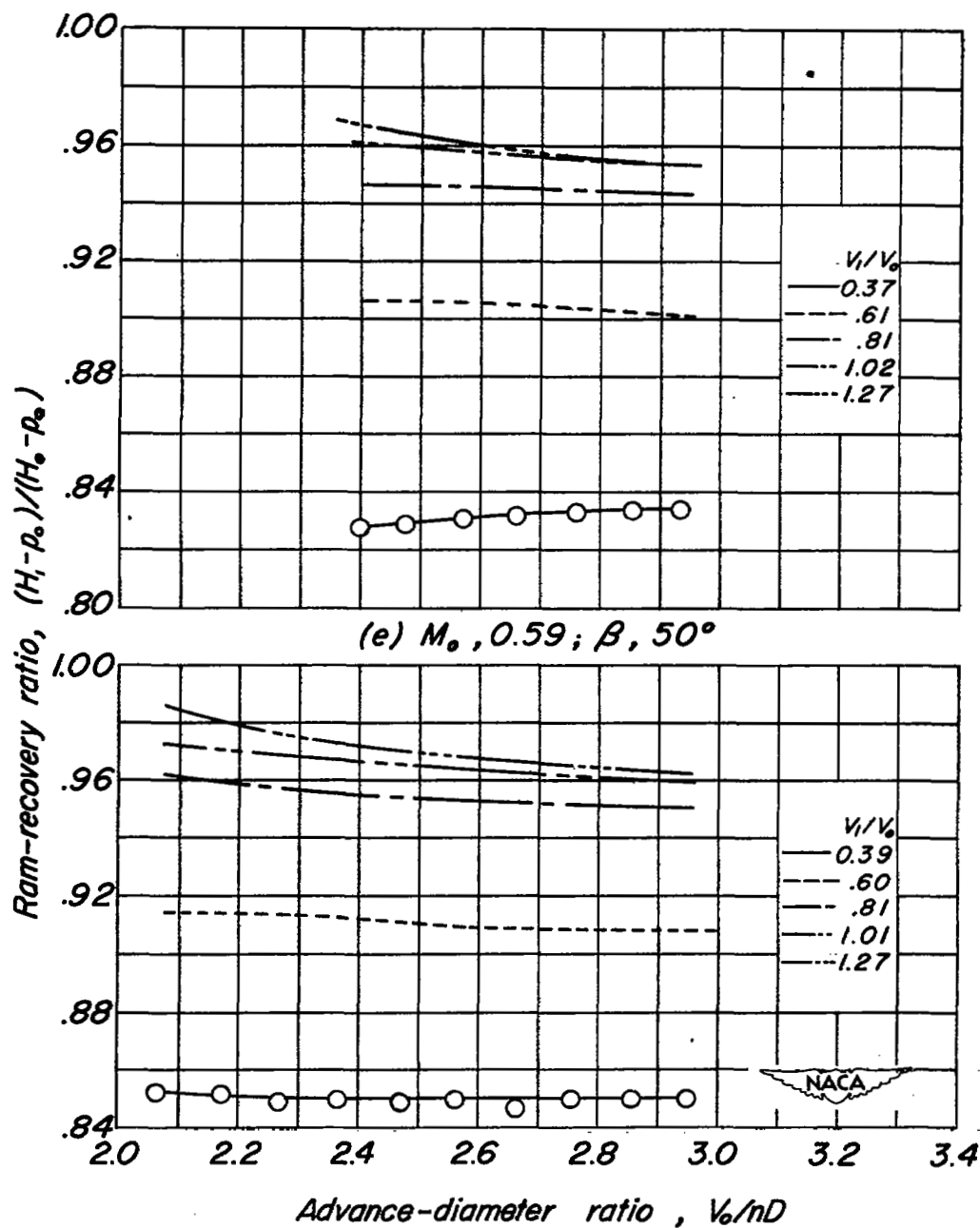
Figure 18.- Continued.

(e) M_0, 0.59; β, 50°

(f) M_0, 0.39; β, 50°

Figure 18.— Continued.

(g) M_o, 0.39; β, 40°   (h) M_o, 0.30; β, 40°   (i) M_o, 0.20; β, 40°

Figure 18.- Concluded.

(a) M_o , 0.83; β, 60°

(b) M_o, 0.79; β, 60°

(c) M_o , 0.69; β, 60°
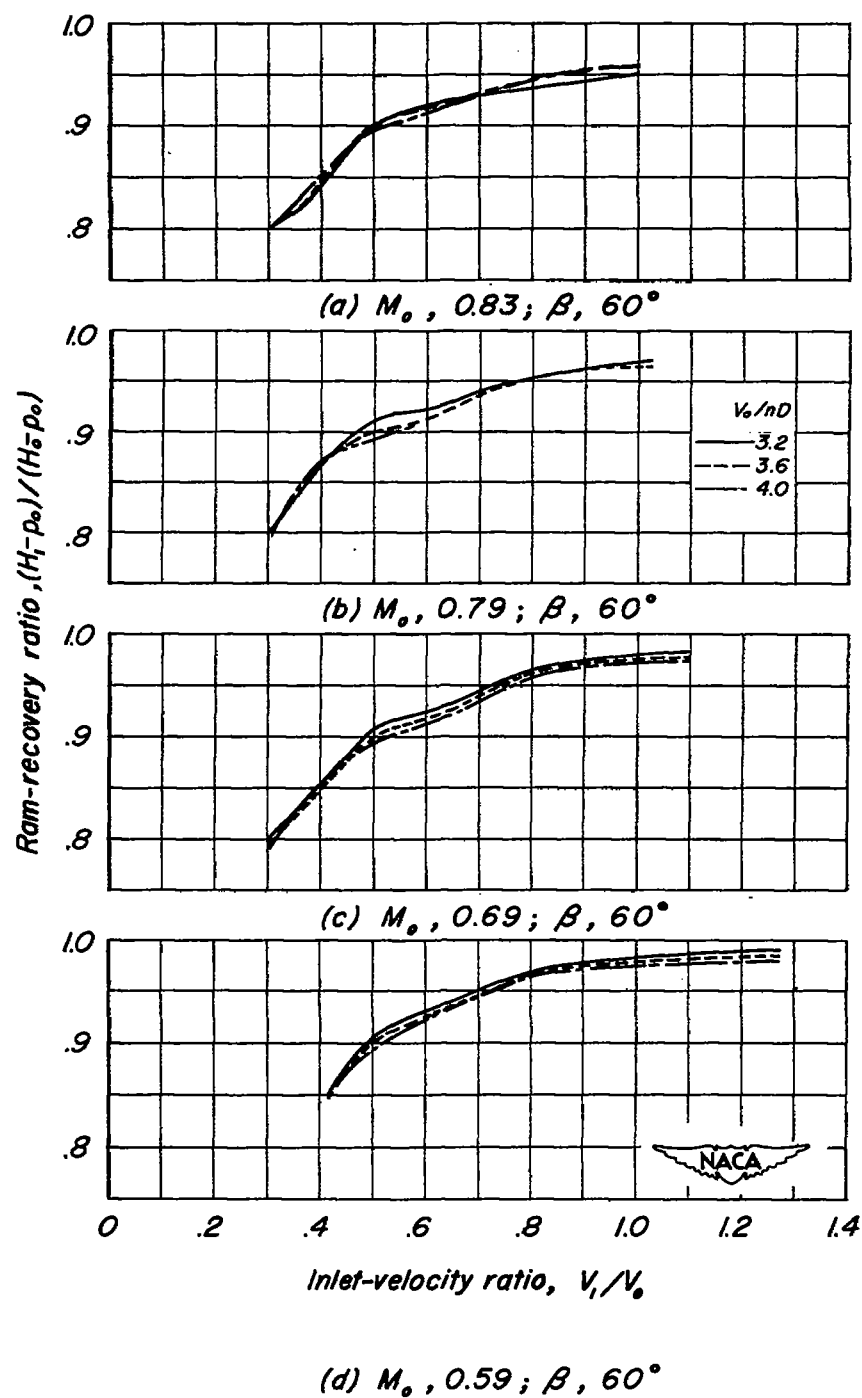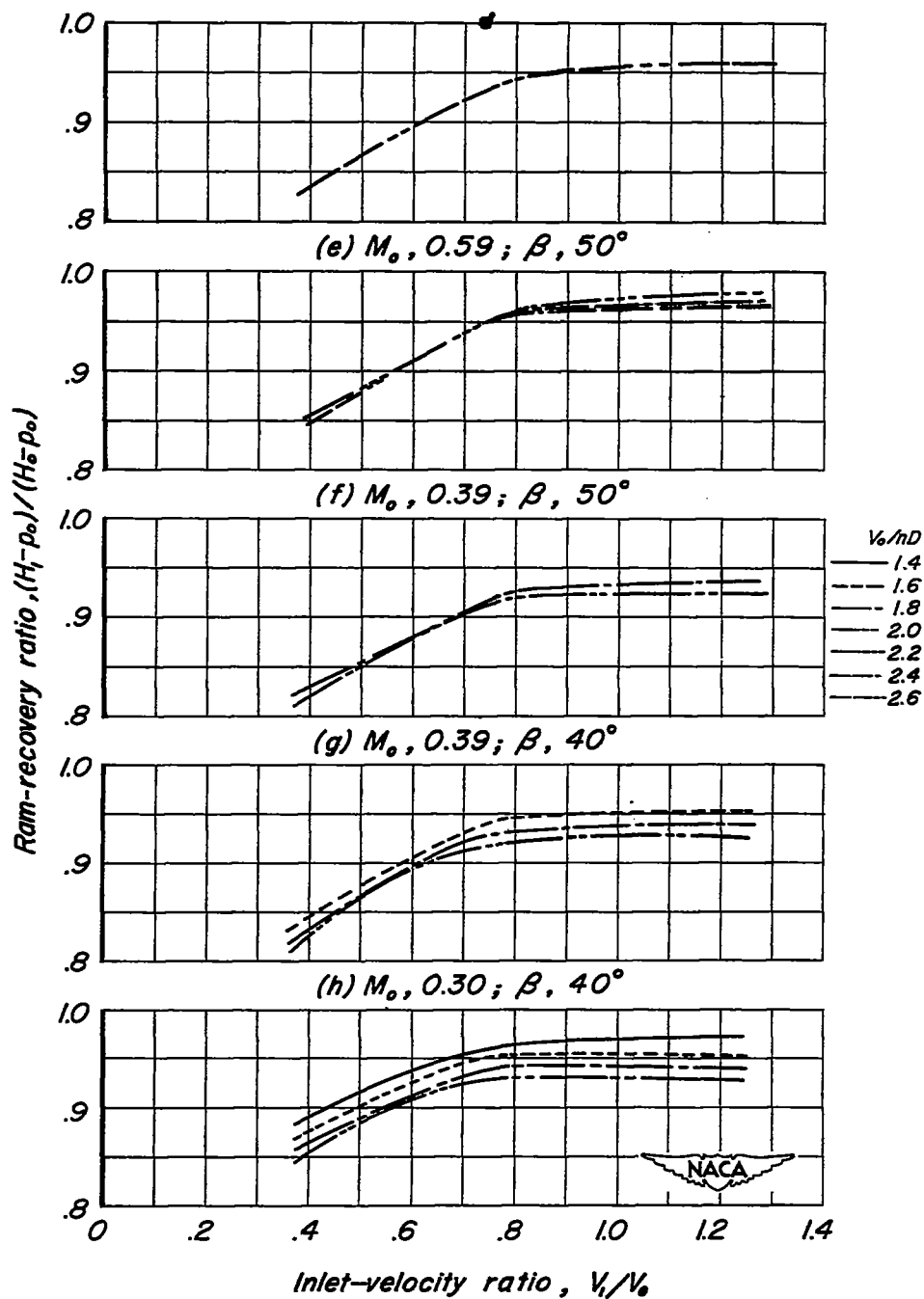
(d) M_o , 0.59; β, 60°
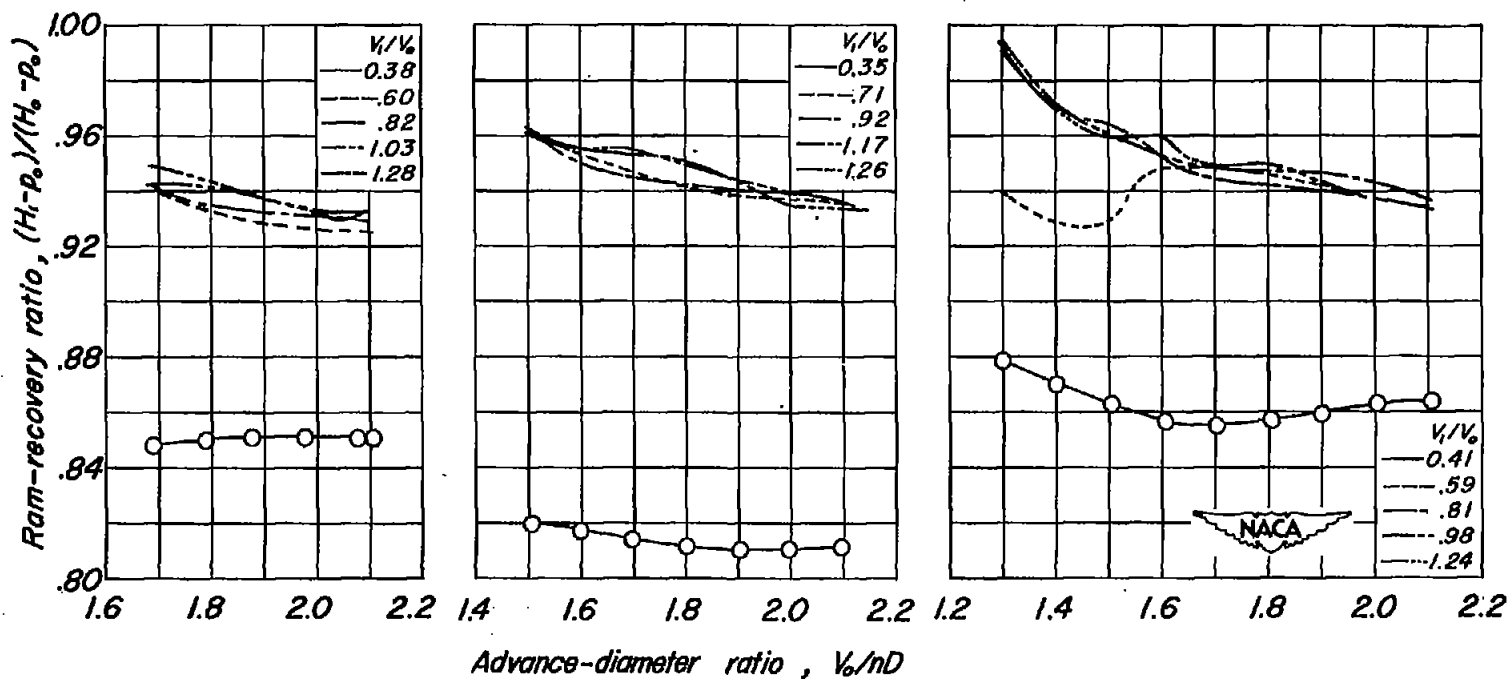
Figure 19.-The variation of the average ram-recovery ratio with inlet-velocity ratio for various advance-diameter ratios, ideal junctures.

(e) M_o, 0.59; β, 50°

(f) M_o, 0.39; β, 50°

(g) M_o, 0.39; β, 40°

(h) M_o, 0.30; β, 40°

Inlet−velocity ratio, V_1/V_o

(i) M_o, 0.20; β, 40°

Figure 19. − Concluded.

(a) M_o , 0.83; β, 60°

(b) M_o, 0.79; β, 60°

(c) M_o, 0.69; β, 60°

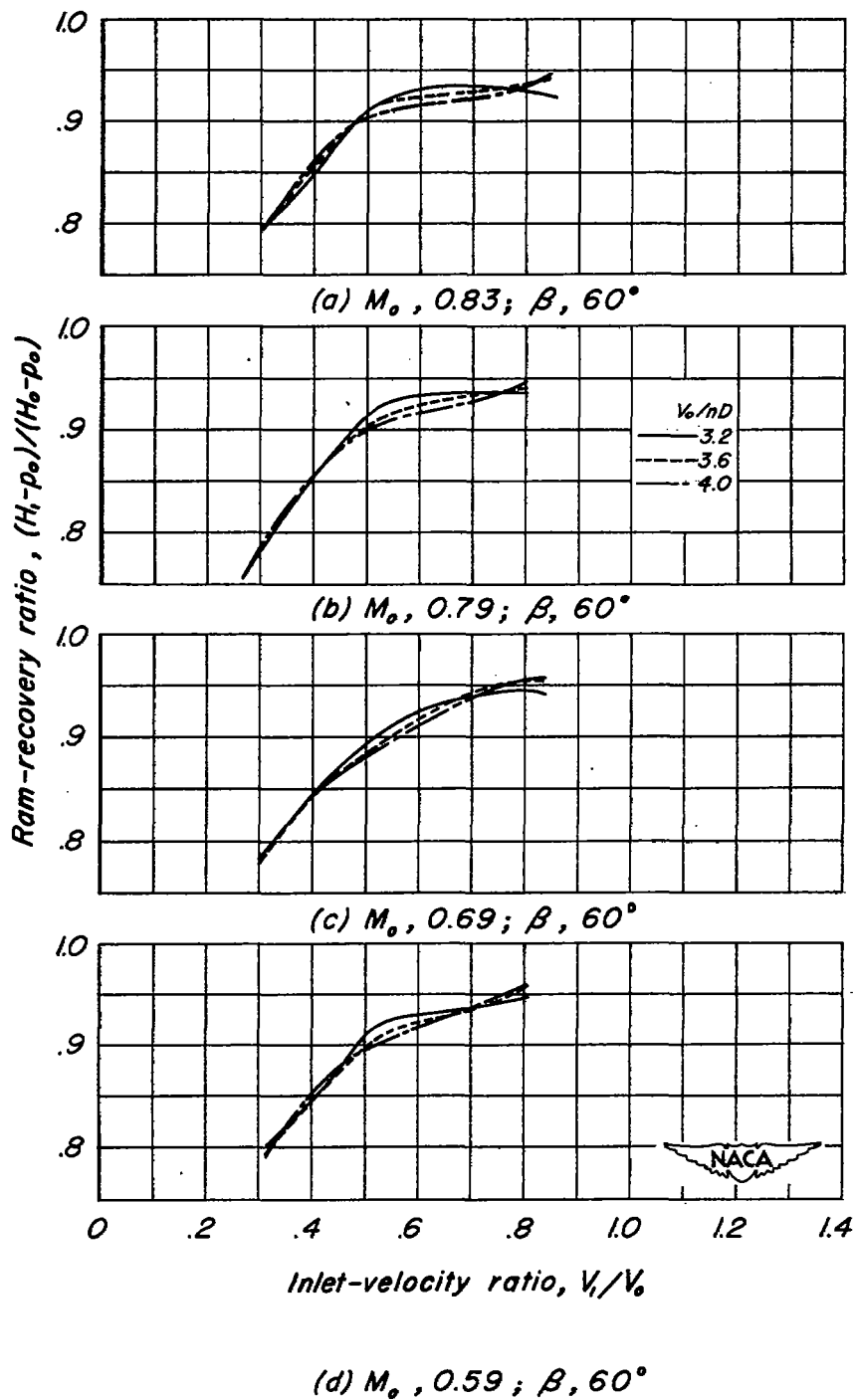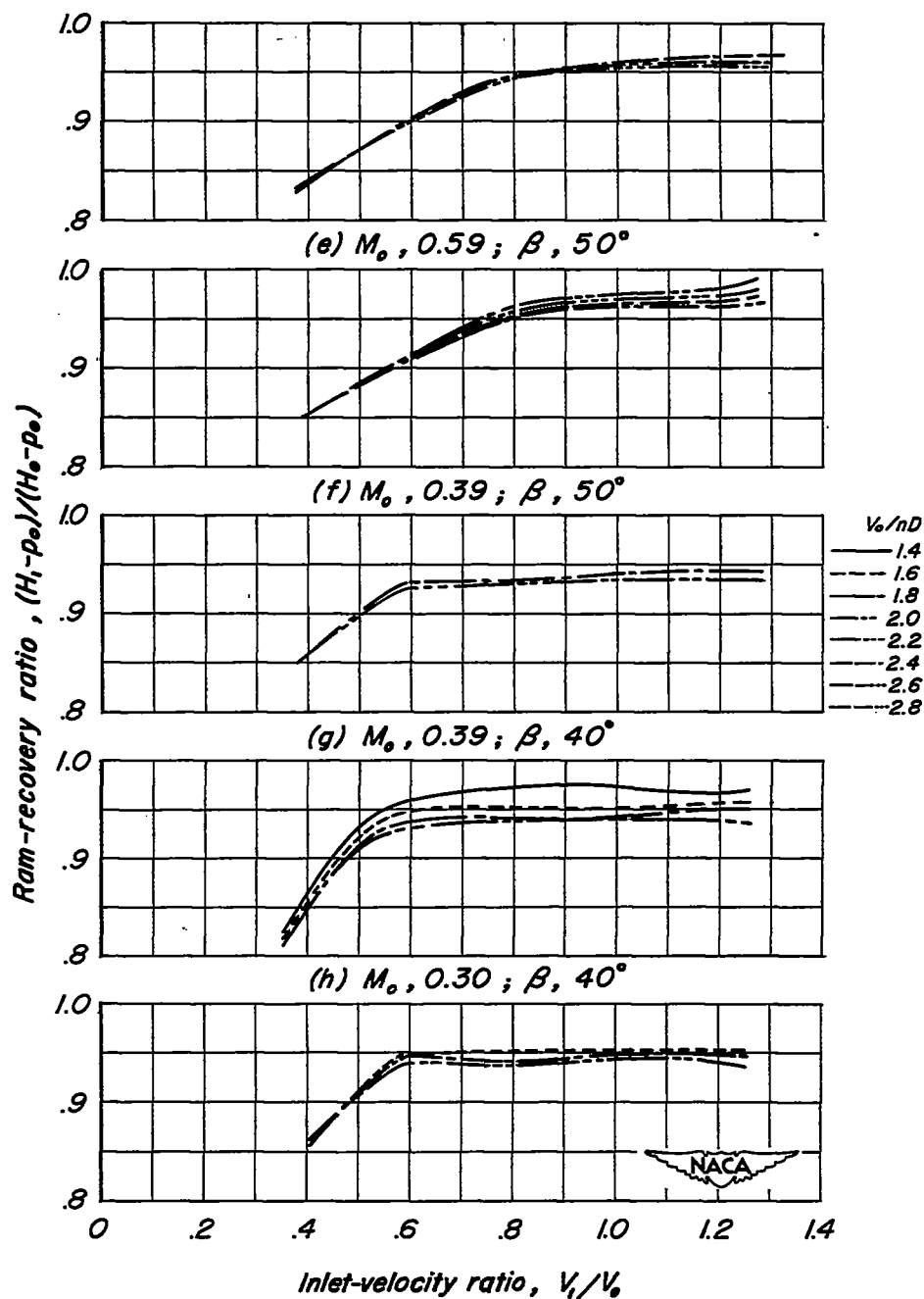Inlet-velocity ratio, V_i / V_o

(d) M_o , 0.59 ; β, 60°

Figure 20.-The variation of the average ram-recovery ratio with inlet-velocity ratio for various advance-diameter ratios, platform junctures.

(e) M_o, 0.59; β, 50°

(f) M_o, 0.39; β, 50°

(g) M_o, 0.39; β, 40°

(h) M_o, 0.30; β, 40°

Inlet-velocity ratio, V_i/V_o

(i) M_o, 0.20; β, 40°

Figure 20.- Concluded.

(a) β, 60°; V_0/nD, 3.7
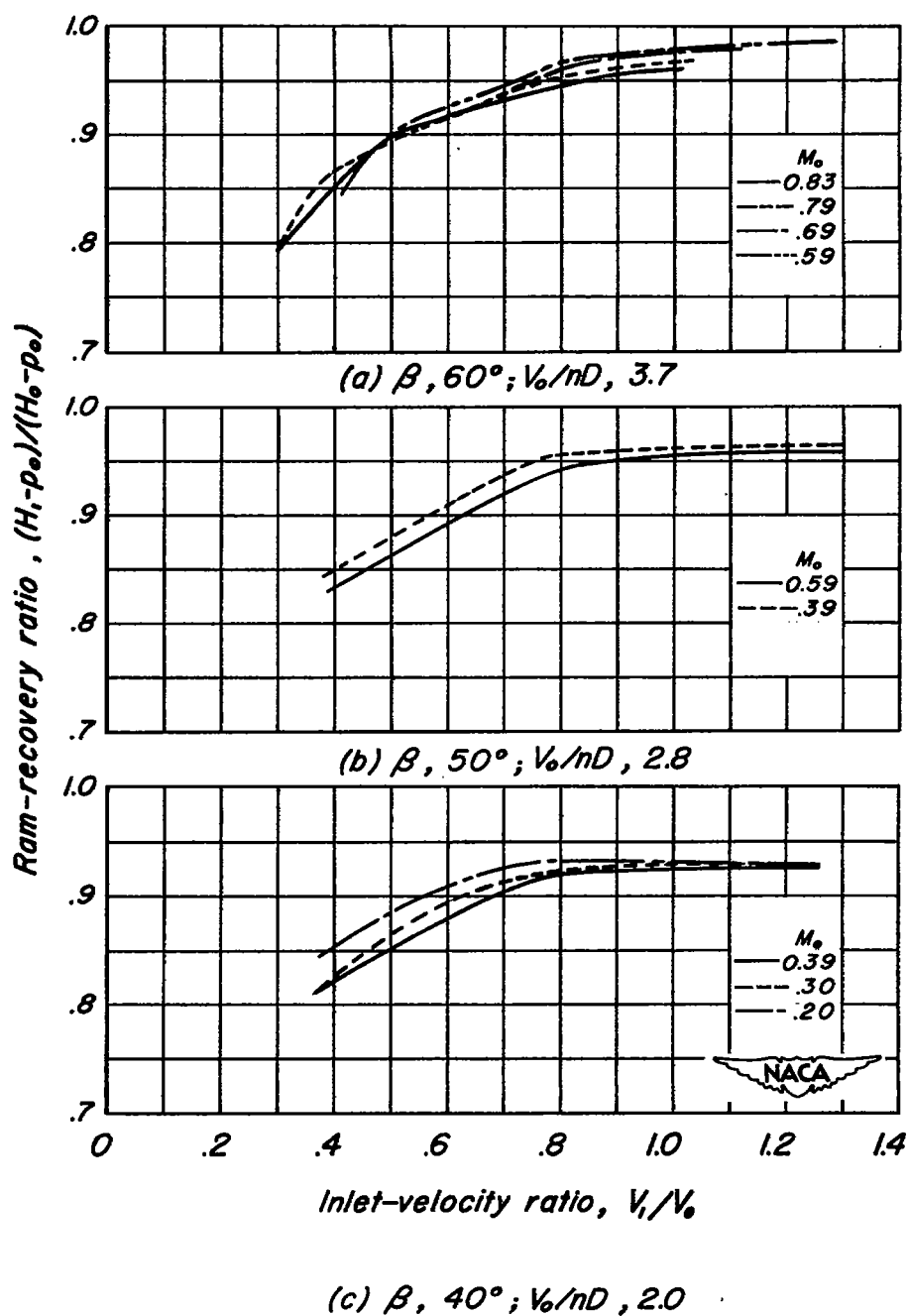
(b) β, 50°; V_0/nD, 2.8

(c) β, 40°; V_0/nD, 2.0

Figure 21.- The variation of the average ram-recovery ratio with inlet-velocity ratio for various Mach numbers, ideal junctures.

(a) β, $60°$; V_0/nD, 3.7
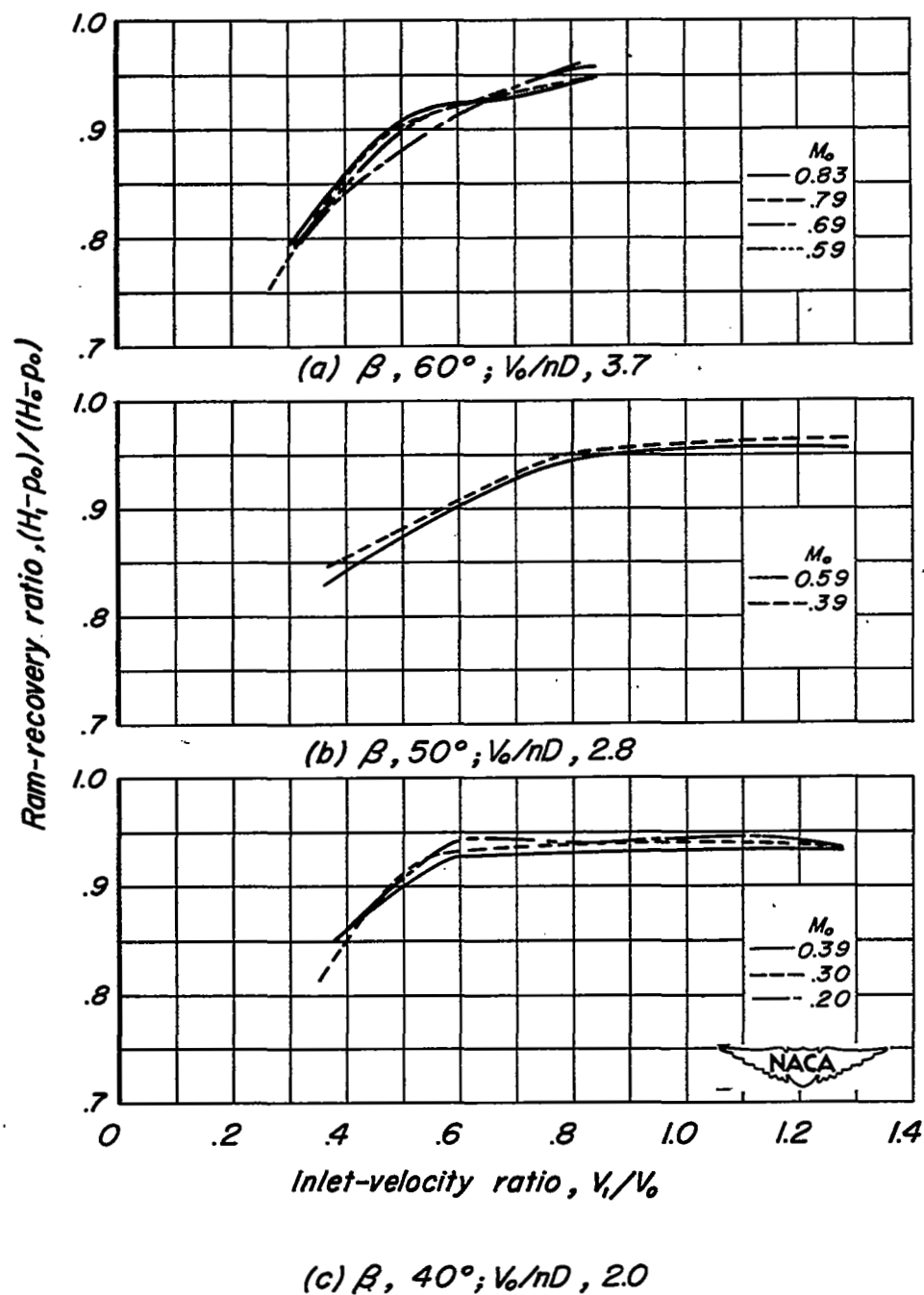
(b) β, $50°$; V_0/nD, 2.8

(c) β, $40°$; V_0/nD, 2.0

Figure 22.–The variation of the average ram-recovery ratio with inlet-velocity ratio for various Mach numbers, platform junctures.

(a) M_0, 0.83; β, 60°

(b) M_0, 0.79; β, 60°

(c) M_0, 0.69; β, 60°
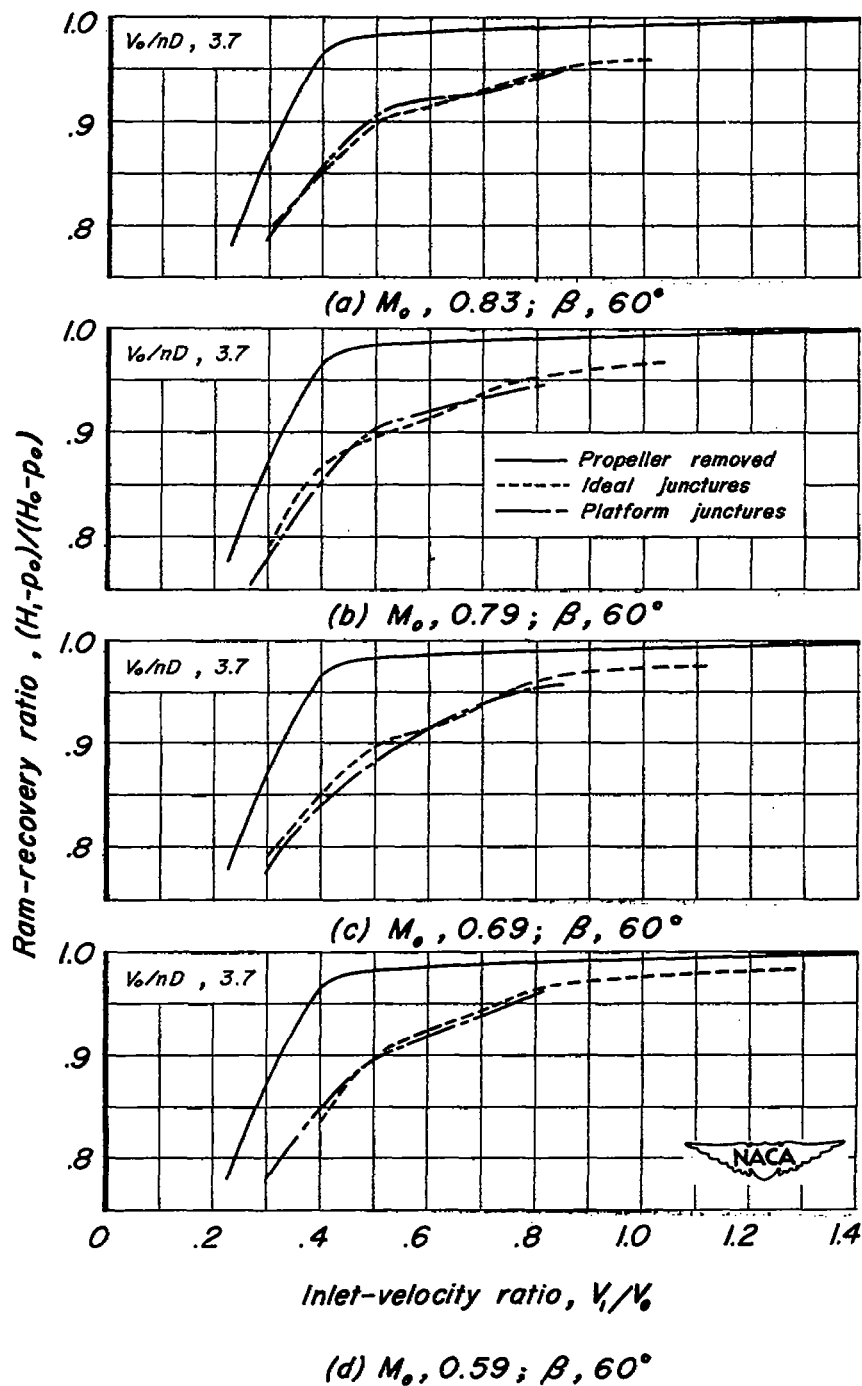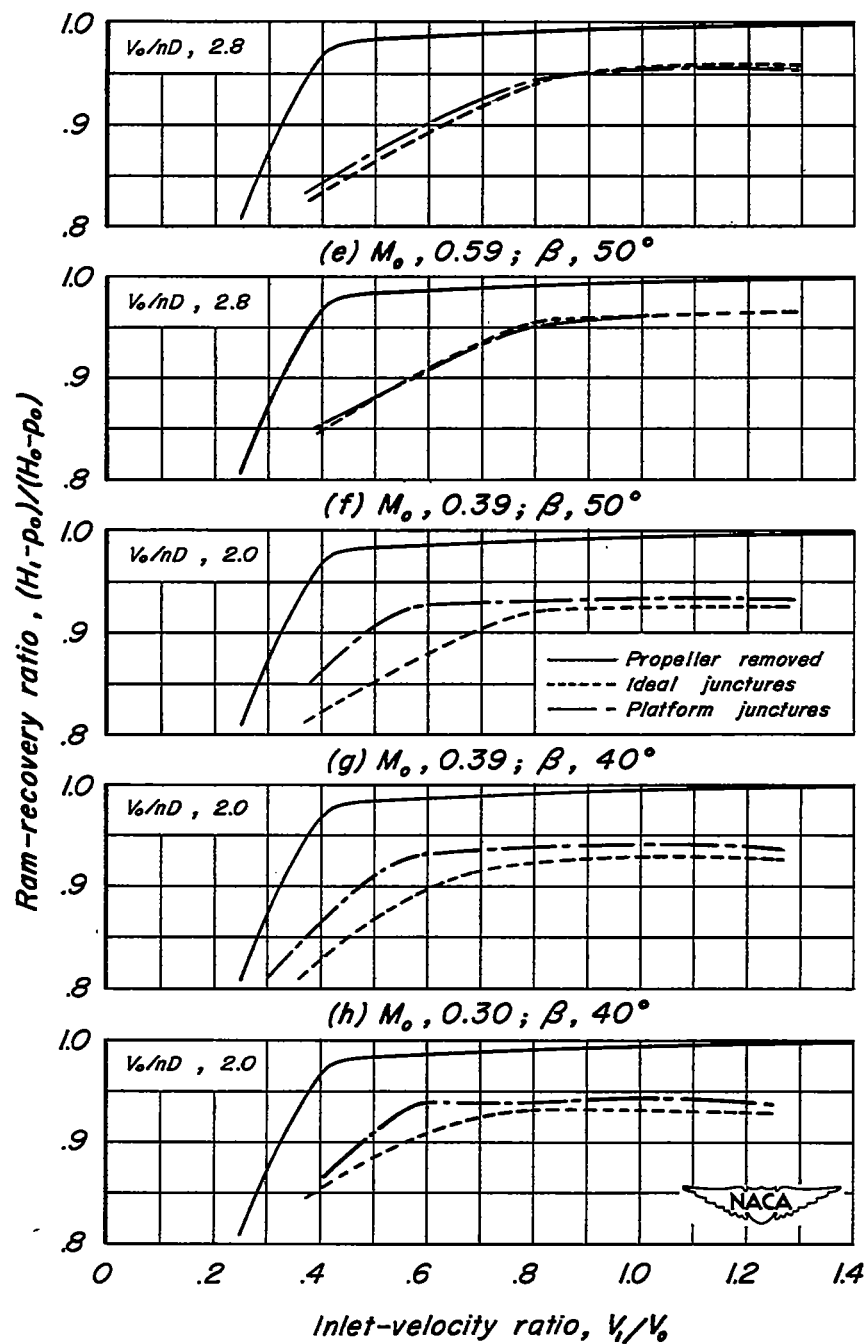
(d) M_0, 0.59; β, 60°

Figure 23.—The variation of the average ram-recovery ratio with inlet-velocity ratio with the propeller removed and with the ideal and platform junctures.

(e) M_o, 0.59; β, 50°

(f) M_o, 0.39; β, 50°

(g) M_o, 0.39; β, 40°

(h) M_o, 0.30; β, 40°

Inlet-velocity ratio, V_i/V_o

(i) M_o, 0.20; β, 40°

Figure 23.-Concluded.